CORROSION CONTROL THROUGH A BETTER UNDERSTANDING OF THE METALLIC SUBSTRATE/ORGANIC COATING/INTERFACE

Agreement No. N00014-79-C-0731

NINTH ANNUAL REPORT
COVERING THE PERIOD
OCTOBER 1, 1987 - SEPTEMBER 30, 1988

Sponsor: Office of Naval Research
Washington, D.C.

Principal Investigator: Henry Leidheiser, Jr.
Co-Investigator: Richard D. Granata

Zettlemoyer Center for Surface Studies
LEHIGH UNIVERSITY
Bethlehem, PA 18015

February 6, 1989

TABLE OF CONTENTS

	Page
FOREWORD	1
Papers Covering Work Supported by ONR and Published during 1987	2
Papers Published during 1988 on Research Not Supported by ONR	3
Solid State NMR Studies of Sodium Ions in A Polybutadiene Matrix	5
Corrosion Inhibition of Steel by Lead Pigments I. The Steel-Lead Galvanic couple in Acetate Solutions	23
Inhibition in the Context of Coating Delamination .	45

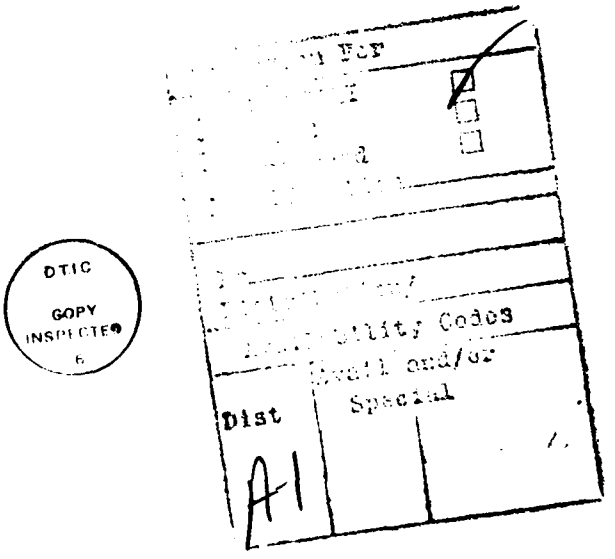

FOREWORD

This report represents the ninth annual and final summary of research carried out under Office of Naval Research Contract No. N00014-79-C-0731. The objective of the research is to obtain a better understanding of the metallic substrate/organic coating/ interface system so that improvements may be made in corrosion control of metals by painting.

Papers published during the period, January 1, 1988 - December 31, 1988, for which ONR provided total or partial financial support are listed chronologically. Papers published during the same period and to which ONR provided no financial support are also listed.

Three summaries of reports submitted for publication representative of work completed during the past year are given. Two of these papers have been accepted for publication and the third has been submitted for publication.

→ Sodium, polybutadiene, Steel, Lead, Acetates, Coatings. (mg/m)

Papers Covering Work Supported by ONR and Published during 1988

"Cathodic Blistering of Two Alkyd Paints," V. S. Rodriguez and H. Leidheiser, Jr., J. Coatings Tech. 60(757), 46-51 (1988).

"Carboxylate Formation at the Interface between a Polyimide Coating and Cobalt," Richard D. Granata, Philip D. Deck and Henry Leidheiser, Jr., Proceedings of the 1987 Tri-Service Conference on Corrosion, Fred H. Meyer, Jr., Editor, U.S. Air Force Academy, CO, May 1987, Vol. II, pp. 280-302 (1988).

"Mechanisms of De-Adhesion of Organic Coatings from Metal Surfaces," H. Leidheiser, Jr., In Proceedings 1985 Tri-Service Conference on Corrosion, December 2-5, 1985, pp. 385-98. Published 1988.

"Positron Implantation and Annihilation in Protective Organic Coatings," Cs. Szeles, K. Süvegh, A. Vértes, M. L. White and H. Leidheiser, Jr., J. Coatings Tech. 60(758), 47-52 (1988).

"Emission Mössbauer Study of the Interface between a Cobalt Substrate and a Polyimide Coating," Attila Vértes, Ilona Czakó-Nagy, Philip Deck and Henry Leidheiser, Jr., Hyperfine Interactions 41, 729-32 (1988).

"Mössbauer Spectroscopic and Electron Microscopic Study of Fe^{3+} Introduced into Alkyd and Epoxy Corrosion Protective Coatings," A. Vértes, A. Cziraki, I. Czakó-Nagy and H. Leidheiser, Jr., J. Electrochem. Soc. 135(9), 2143-46 (1988).

"Chemistry of the Metal-Polymer Interface," Henry Leidheiser, Jr., and Philip D. Deck, SCIENCE 241, September 2, 1988, 1176-81 (1988).

"Positron Annihilation in Corrosion Protective Polymeric Coatings, II," Cs. Szeles, A. Vértes, M. L. White and H. Leidheiser, Jr., Nuclear Instruments and Methods in Physics Research A271, 688-92 (1988).

"Ion Transport through Protective Polymeric Coatings Exposed to An Aqueous Phase," Henry Leidheiser, Jr., and Richard D. Granata, IBM J. Res. Develop. 32(5), September 1988.

"Positron Lifetime Studies of Organic Coatings," K. Süvegh, Cs. Szeles, M. L. White, A. Vértes, H. Leidheiser, Jr., Proceedings of the European Meeting on Positron Lifetime Studies of Organic Coatings, Wernigerode, West Germany, March 23-27, 1987.

"Water Disbondment Characterization of Polymer Coating/Metal Substrate Systems," S. J. Spadafora and H. Leidheiser, Jr., JOCCA 71(9), 276-85 (1988).

Papers Published during 1988 on Research Not Supported by ONR

"Applications of Mössbauer Spectroscopy to Studies of Electrodeposits and the Chemistry of Metal Surfaces," Henry Leidheiser, Jr., J. Electrochem. Soc. 135(2), 5C-11C (1988).

"Factors Affecting the pH within Carbon Steel Crevices," H. Leidheiser, Jr., R. D. Granata, G. Fey and M. Ingle, Corrosion Science 28(6), 631-32 (1988).

"Epoxy Powder Coatings for Conformal Coating and Corrosion Protection of Copper," R. D. Granata, P. Deck, and H. Leidheiser, Jr., J. Coatings Tech. 60(763), 41-51 (1988).

"Metal-Ion Modified Zinc Anodes for Alkaline Battery Studies, " R. D. Granata, J. W. Catino, and H. Leidheiser, Jr., Proceedings of 33rd International Power Sources Symposium, Cherry Hill, NJ, June 13-16, 1988.

SOLID STATE NMR STUDIES OF SOIDUM IONS IN A POLYBUTADIENE MATRIX

Rachel Turoscy, Henry Leidheiser, Jr., and James E. Roberts

Note: This paper has been submitted for publication in the JOURNAL OF PHYSICAL CHEMISTRY.

ABSTRACT

Sodium ions were implanted into polybutadiene by cathodic polarization of polybutadiene-coated copper in 0.5M aqueous solutions of NaCl, NaBr, and NaI. The chemical environment of the implanted sodium was studied utilizing Magic Angle Sample Spinning (MASS) solid state NMR techniques. The sodium ions were present in two types of environments when exposed to water. The majority was present as hydrated ions within the polymer and was represented by a sharp component of the ^{23}Na NMR spectrum. A smaller quantity was present as a constrained species represented by a broad component of the ^{23}Na NMR spectrum. When dry, the sodium ions associated with carboxyl groups present in the matrix.

INTRODUCTION

There is ample evidence that an important failure mechanism of protective organic coatings involves ion passage through the coating. For example, pathways for ion transit permit coupling of anodic and cathodic regions through the coating and the electrolyte to which the coated metal is exposed. Ion migration is especially detrimental in the case of failures based on cathodic delamination (1), in which cations pass through the coating and develop strongly alkaline solutions under the coating that lead to bond rupture between the coating and the metal. Ion transport through the coating may also be responsible for dendrites that develop under some circumstances when polyimide coatings on copper are utilized for insulation in high temperature transformers (2).

Research, done primarily by Mills (3,4,5), has suggested that there are two mechanisms by which cations migrate within a polymeric coating. Some portions of polymeric free films have resistances greater than 10^{12} ohm·cm^2 and the magnitude of these resistances is inversely proportional to the conductivity of the electrolyte to which the free film is exposed. Other portions of the free film have resistances of 10^7 ohm·cm^2 or less and the resistances vary directly with the conductivity of the electrolyte to which the free film is exposed. Mayne and Mills (3) have characterized the former regions as I-type and the latter as D-type. It is conjectured that I-type behavior is characteristic of a polymer film (or coating) having no continuous charge pathways; ions conducting the charge migrate through the polymer matrix by a method which might be termed a random walk. Films with D-type behavior contain conductive pathways through which the ions move. It is probable that these pathways are filled with aqueous phase when the film (or coating) is immersed in an electrolyte. Corrosion of a metal such as

iron occurs at the point where the conductive pathways intersect the metal surface. It has been the experience of our laboratory that coatings with impedances of less than 10^9 ohm·cm^2 at low frequencies do not adequately protect the substrate metal from corrosion (6).

A substantial interest has developed in trying to understand the chemical nature of ions when present in both unpigmented and pigmented coatings. Our work to date has been limited to cations because of our prior experience that applied cathodic potentials increase the rate of cation migration through the coating (7). We have recently utilized emission Mössbauer spectroscopy to study the state of Sn(IV) and Co(II) in alkyd, epoxy, and polybutadiene coatings (8,9). The results of these studies were provocative but the limited number of ions that can be studied by the emission Mössbauer technique prompted us to seek another spectroscopy that would be useful for studying a range of ions, both cations and anions.

The utility of solid state Magic Angle Sample Spinning (MASS) NMR techniques to studies of a wide variety of ionic species and the ability of the technique to generate information about the chemical environment of an ion encouraged us to explore this method. We report herein studies of the nature of the sodium ion when incorporated into polybutadiene coatings on copper by means of an applied cathodic potential. Polybutadiene was selected because of our extensive experience with this coating material (10). Sodium was selected because it is important in several types of protective coating deterioration, it is a ubiquitous ion, and the NMR sensitivity is reasonably high (11).

EXPERIMENTAL

All chemicals were reagent grade and used without further purification. Uncured polybutadiene was obtained from Dupont. 3" x 3" Fisher Scientific 1/32" copper foil sheets, were spin coated with polybutadiene and cured in air at 190°C for 20 min. The coating thickness was typically 25 μm. A 0.1 mm diameter defect was made in the center of the coated sample which was then mounted in an "O" ring apparatus. The electrolytes used were 0.01-5M NaCl, 0.5M NaBr, and 0.5M NaI. The samples were cathodically polarized (12,13,14) at a potential of -0.8v vs Ag/AgCl.

The coating was removed from the substrate after complete delamination of the exposed area (35.2 cm^2) and washed in a constant stream of distilled water for 2 min. The delaminated section was packed into a 7 mm sapphire rotor from Doty Scientific, Inc., for NMR analysis by Bloch decay (15) or Hahn echo (16) experiments with a repetition time of 2 sec. The ^{23}Na MASS NMR spectra were recorded at 79.37 MHz on a General Electric NMR Instruments Model GN-300 spectrometer equipped with a Doty Scientific probe. Spin-lattice relaxation times, T_1, were determined by the 180-τ-90 inversion recovery pulse sequence (17). T_2, the spin-spin relaxation time, was determined by the Carr-Purcell-Meiboom-Gill spin echo method (18,19). T_1 and T_2 values are reported accurate to ±10%. Maximum radio frequency field strengths for ^{23}Na, ^{13}C, and ^{1}H were 5.0 mT, 7.0 mT and 2.0 mT with a 2 sec repetition time for cross polarization experiments (20). The spinning rate for each ^{23}Na spectrum was between 2 and 3 kHz, while ^{13}C spectra were obtained at 8.5 kHz on a 5 mm fast spinning probe from Doty Scientific, Inc. Chemical shifts for ^{13}C and ^{23}Na spectra are reported with an accuracy of ±.2 ppm relative to external adamantane (21) and solid NaCl.

RESULTS AND DISCUSSION

Table 1 lists the chemical shifts for various sodium salts, aqueous NaCl (0.01-5M), aqueous NaBr (0.5M), aqueous NaI (0.5M), and aqueous $NaC_2H_3O_2$ (0.5M) relative to solid NaCl. These salts were chosen in an attempt to characterize possible chemical environments of the sodium ion within the polybutadiene matrix. Of special note is the position of the aqueous sodium halides, independent of concentration at -7.4 ppm relative to solid NaCl.

Table 1
Chemical Shifts of Various Sodium Salts

Compound	Chemical Shift* (ppm)
NaBr	-2.3
Na_2CO_3	-4.4
NaCl solution (0.01M)	-7.4
NaCl solution (0.1M)	-7.4
NaCl solution (0.5M)	-7.4
NaCl solution (5M)	-7.4
NaBr solution (0.5M)	-7.4
NaI solution (0.5M)	-7.4
$NaC_2H_3O_2$ solution (0.5M)	-7.4
$NaHCO_2$	-7.5
NaI	-9.8
$NaHCO_3$	-13.4
$NaC_2H_3O_2$	-17.5,-17.8,-23.0
$Na_2C_2O_4$	-42.1

*Solid NaCl salt as external reference

Figure 1 shows the NMR spectra for the sodium ions incorporated into polybutadiene after cathodic polarization in 0.5M solutions of NaCl (1a), NaBr (1b), and NaI (1c). The single peak in each of these spectra has a -7.4 ppm chemical shift consistent with the chemical shift of the aqueous sodium halides seen in Table 1. The feature arises from Na ions in a hydrated state, probably within aqueous volumes in the polybutadiene matrix. The weak features found at 9 ppm and -23 ppm are rotational side bands, separated from the strong central line by the spinning speed.

An ideal Lorentzian line shape has a value of 2.65 for the ratio of the width at 1/8 height, $\nu_{1/8}$, to the width at half height, $\nu_{1/2}$. The value of this ratio for the ^{23}Na NMR spectrum in Figure 1 is 3.8 indicative of the fact that the signal is the sum of at least two Lorentzians (22). Further resolution of the ^{23}Na NMR spectrum was also obtained through application of the 90-τ-180 pulse sequence which generates a Hahn echo. This experiment helps to eliminate line broadening from instrumental probe ringdown. Figure 2 shows the NMR spectra for sodium in polybutadiene after polarization in 0.5 M NaCl as determined by Bloch Decay (2a) and by the Hahn Echo pulse sequence (2b). The line width of the peak in the Hahn Echo spectrum (2b) when compared to the Bloch decay (2a) shows some narrowing. However, not all of the non-Lorentzian character was eliminated by the Hahn Echo experimental. The ratio of $\nu_{1/8}/\nu_{1/2}$ for the Hahn Echo spectrum was 2.8 indicating the existence of multiple environments for sodium in the polybutadiene matrix.

The Carr-Purcell-Meiboom-Gill pulse sequence was used to determine T_2 relaxation time limits for each component in the main feature. Figure 3 is the graphical result of the natural logarithm of the echo intensities as a function of time τ. Two distinct exponential decays are resolved from this plot. The shorter τ times yield a T_2 of 9 msec ($\nu_{1/2}$ = 35 Hz) while the longer τ values result in a T_2 of 35 msec ($\nu_{1/2}$ = 9 Hz). The 35 msec T_2 value

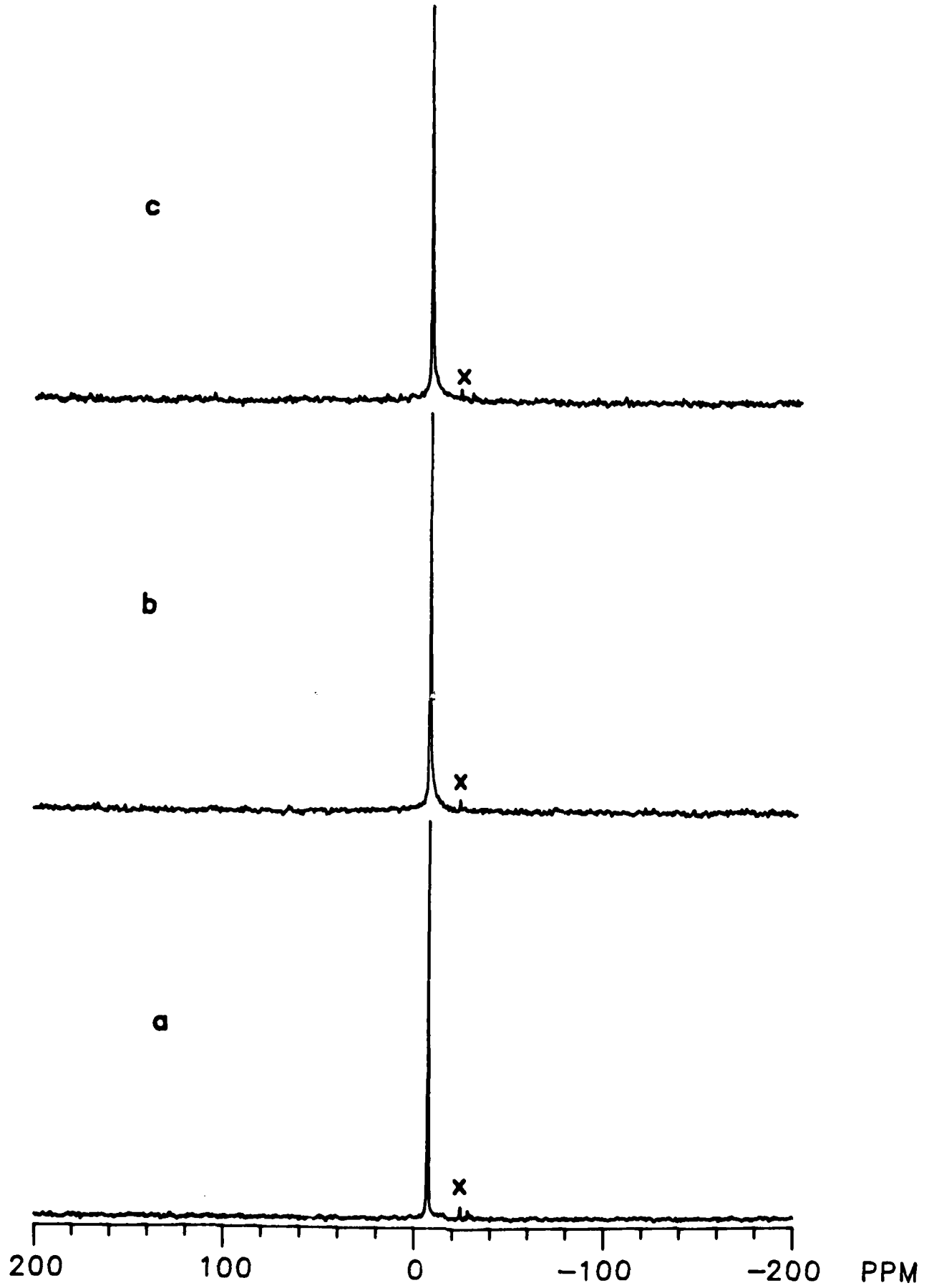

Figure 1. ^{23}Na MASS NMR spectra of polybutadiene cathodically polarized in (a) 0.5M NaCl, (b) 0.5M NaBr, and (c) 0.5M NaI. X indicates rotational side band.

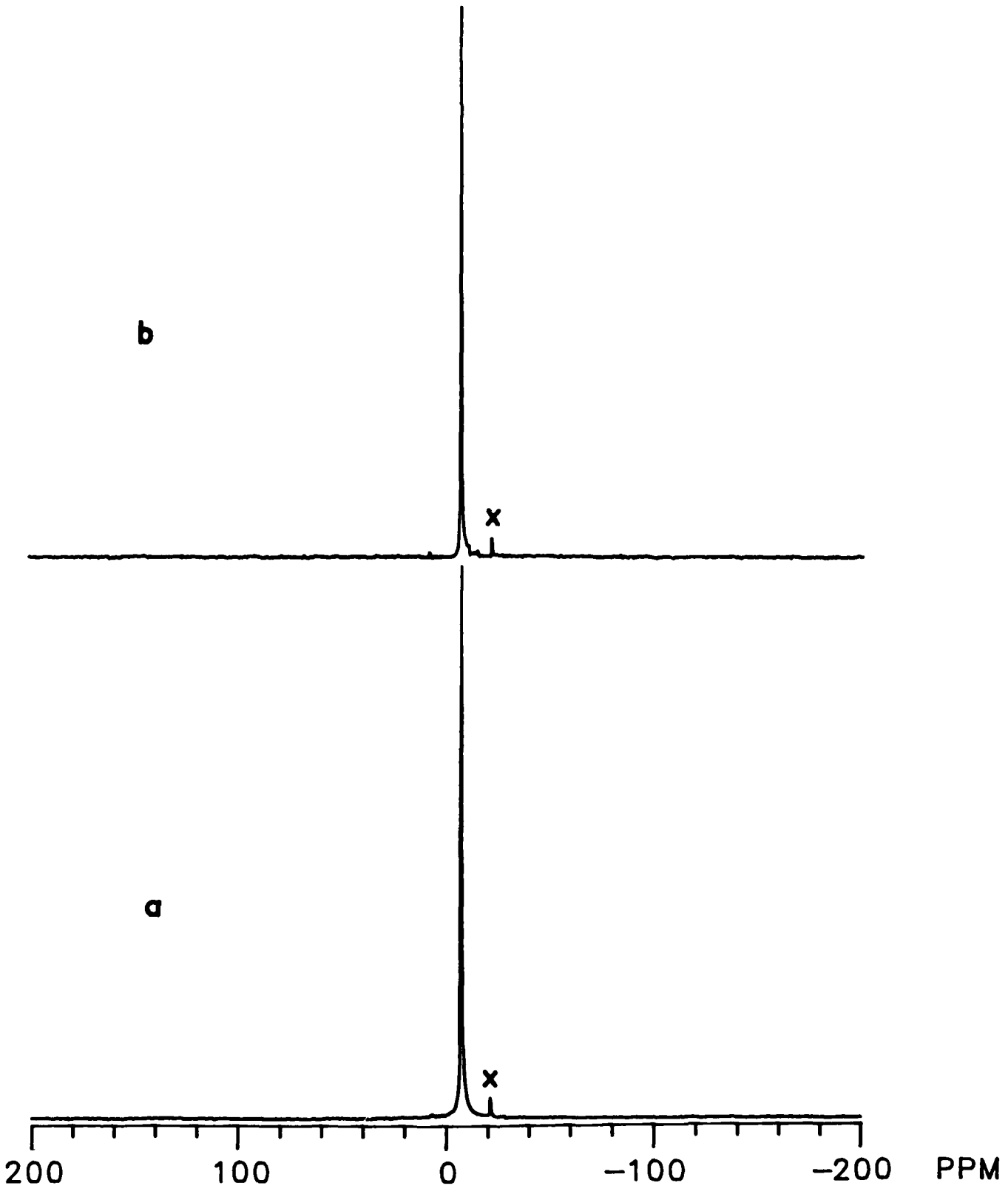

Figure 2. ^{23}Na MASS NMR spectra of polybutadiene cathodically polarized in 0.5M NaCl as determined by (a) Bloch Decay and (b) the Hahn echo pulse sequence. X indicates rotational side band.

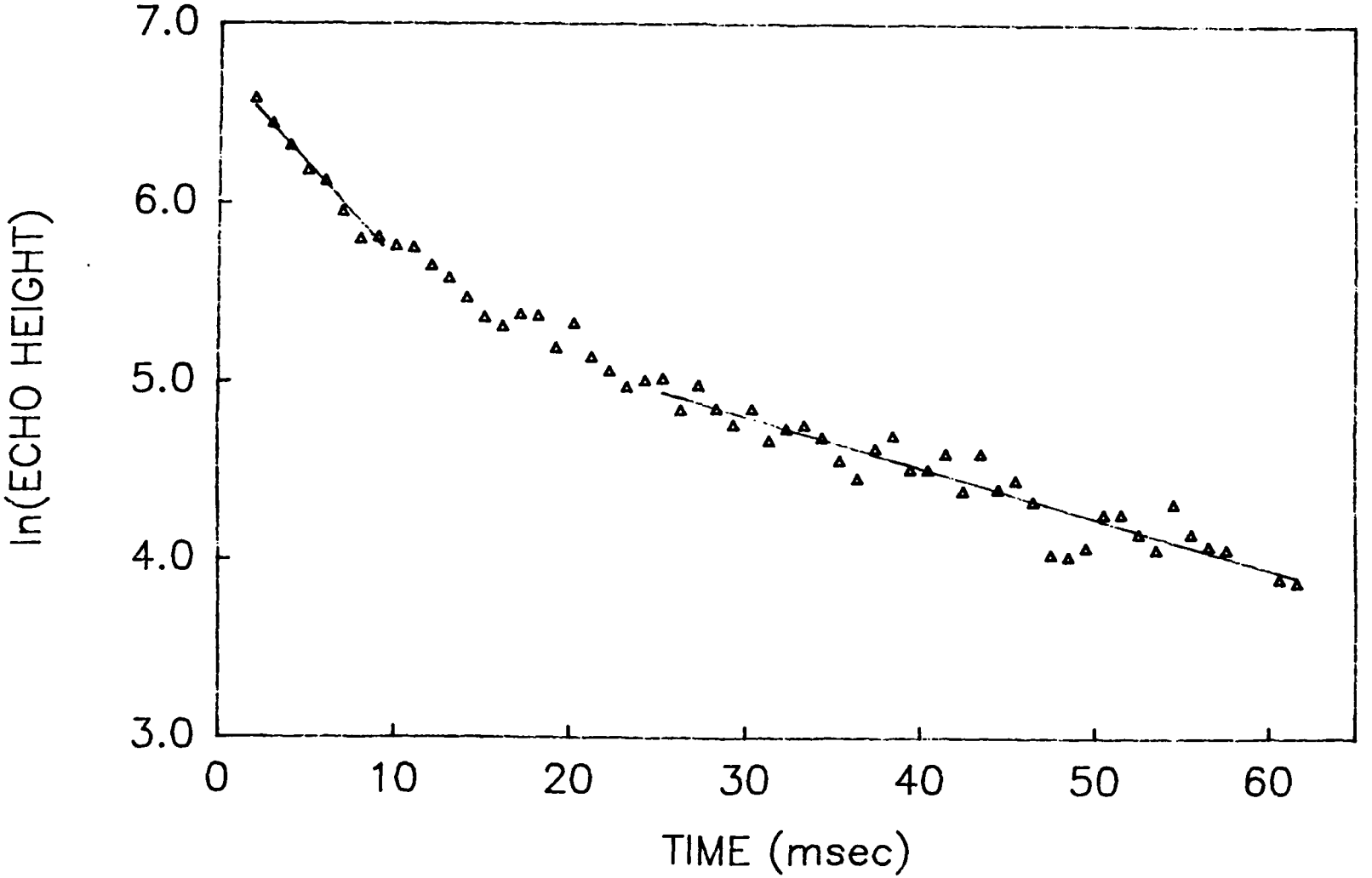

Figure 3. Graphical analysis of the Carr-Purcell-Meiboom-Gill pulse sequence determining T_2 relaxation times for sodium in polybutadiene.

is approximately the same as the T_2 time of 40 msec measured for sodium in 0.5M NaCl.

The T_2 data and non-Lorentzian line shape indicate that the ^{23}Na NMR spectrum is composed of different components. The sharp component in the ^{23}Na NMR spectrum represents the majority of the ions in the polybutadiene. These ions are a very mobile hydrated species and have a T_1 relaxation time of 60 msec as measured by inversion recovery. This value is not significantly different from the 65 msec T_1 time measured for sodium in 0.1 M and 0.5 M aqueous NaCl solutions.

The sodium ions represented by the underlying broad component cannot be categorized into a single environment. This feature consists of multiple broad lines which vary in width and intensity and are representative of other environments in the matrix. Deconvolution of experimental spectra into component lines did not yield a unique solution, even with resonances consistent with the observed T_2 values. This small percentage of sodium ions is presumed to be hydrated but to have less overall mobility. The inhibition of movement by the polymer matrix leads to line broadening possibly as a result of residual quadrupolar interactions which add breadth to the NMR spectrum. The limit of the T_2 relaxation time from Figure 3 is 9 msec for this species of ions. Direct measurement of T_1 relaxation time for the broad features by inversion recovery was not possible due to the position and low intensity of the component underneath the sharp feature.

Sodium ions in an aqueous environment within the polymer is further evidenced by Figure 4. Figure 4a is the ^{23}Na MASS NMR spectrum for a polybutadiene sample cathodically polarized in 0.5M NaI that was dried for 1 week with a silica gel desiccant. Figures 4b and 4c show the ^{23}Na NMR spectra obtained after addition of 1 μl and 15 μl of distilled water, respectively.

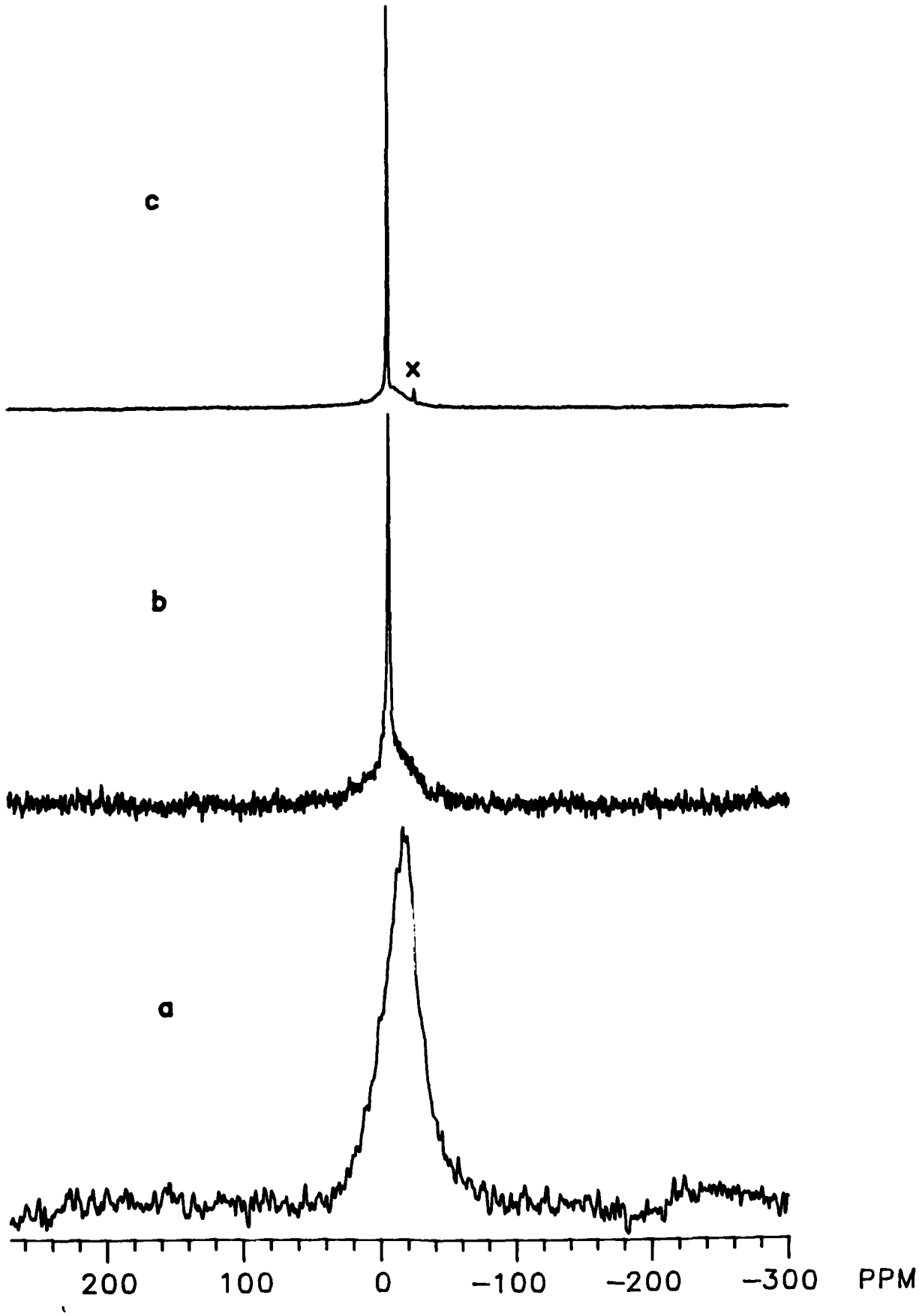

Figure 4. ^{23}Na MASS NMR spectra of polybutadiene cathodically polarized in 0.5M NaI with (a) no water, (b) 1 µl distilled water, and (c) 15 µl distilled water. X indicates rotational side band.

The ^{23}Na NMR spectrum of the dried polybutadiene ($\nu_{1/2}$ = 2700 Hz) shows a -13 ppm (±5 ppm) chemical shift suggestive of Na-oxygen coordination as inferred from similar chemical shifts of solid sodium bicarbonate (see Table 1). Other dehydrated polybutadiene samples which were polarized in NaCl and NaBr had chemical shifts of -17 and -18 ppm (±5 ppm) in line with Na-oxygen coordination in carboxylate groups (vide infra). The sodium ions associate with these sites only when the polymer is dehydrated. Infrared spectroscopic studies of polybutadiene by Deck (23) showed the presence of carboxylate and ester groups in oxidatively cured polybutadiene. T_1 for the Na species within the dehydrated matrix was determined to be greater than 1000 sec.

The NMR spectrum in Figure 4b ($\nu_{1/2}$ = 120 Hz) shows that the introduction of as little as 1 μl water to the sample shifts the peak back to -7.4 ppm. Increasing the amount of water to 15 μl (Figure 4c, $\nu_{1/2}$ = 25 Hz) allows more Na ions to move freely in the aqueous rich volumes after being constrained in the matrix by the drying process. The increased mobility is demonstrated by the decreasing linewidth as water is added. Saturation of the sample occurs after approximately 60 μl of water; the width of the spectrum at half height is 12 Hz (T_1 = 60 msec). Table 2 shows the intensity of the sharp component in proportion to the percentage of water in the system.

Table 2. Peak Height Variation with Water Added

WATER ADDED (μl)	% WATER*	HEIGHT INCREASE
0	0.0%	1x
1	0.6%	1.5x
15	9.9%	8.5x
60	39.6%	12x

* Amount of water added relative to weight of polybutadiene.

Figure 5 shows the ^{13}C spectra for cured polybutadiene (5a) and cured polybutadiene that was cathodically polarized in a 0.5M NaCl solution (5b). Protonated and unprotonated carbon peak assignments were resolved by interrupted decoupling during the cross polarization experiment (24). The small peaks between 210 and 170 ppm represent carbon as carbonyls in ketones and COOR or COOH groups, respectively. The unsaturation of the polybutadiene backbone gives rise to the peaks at 114, 130, and 140 ppm. The majority of the aliphatic carbon constituents are represented by the strong broad peak at 32 ppm. The broad doublet stretching from 75 to 85 ppm represents a protonated carbon most likely in a CHOH arrangement.

Comparison of these spectra shows that sodium ion incorporation by cathodic polarization does not greatly affect the polymer matrix. The spectrum for the polarized sample shows a 2.3x height increase in features from 170-210 ppm indicative of increased carbonyl content, and a 1.5X height increase for the 75-85 ppm feature. This result is consistent with further polymer oxidation caused by the highly alkaline environment produced at the polybutadiene/copper interface during the polarization process. The increased carbonyl content leads to further sodium-carboxylate bond formation when the sample is dehydrated. However, the NMR spectrum does not reveal the specific location in the matrix where the oxidation occurred (i.e. bulk or interface) and the specific sites where the bond formation takes place in the polybutadiene.

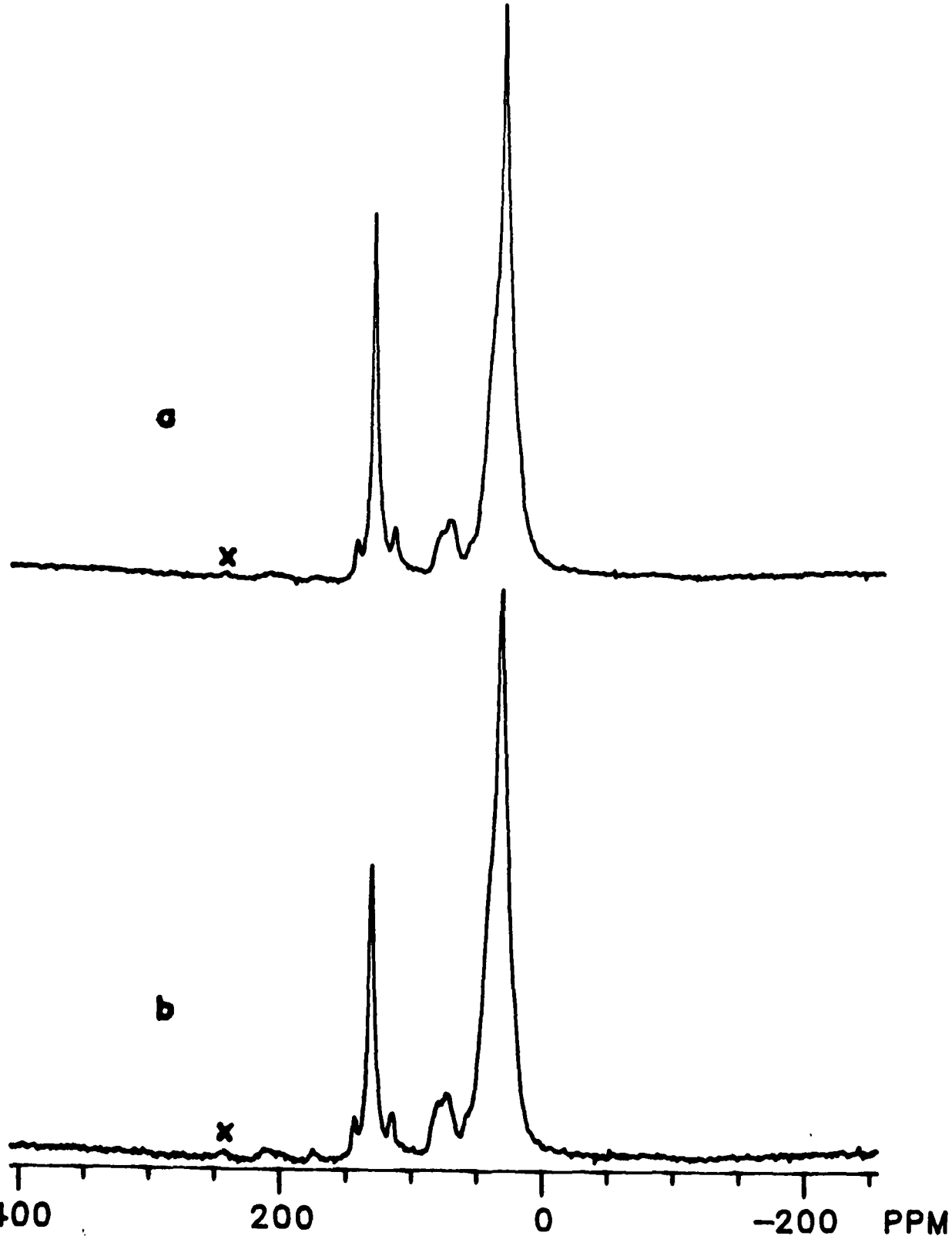

Figure 5. ^{13}C MASS NMR spectra of (a) cured polybutadiene and (b) cured polybutadiene cathodically polarized in 0.5M NaCl. X represents rotational side band observed at the spinning speed of 8.5 kHz.

CONCLUSIONS

Sodium ions exist in three chemical environments within cathodically polarized polybutadiene coatings. When hydrated, the solid state ^{23}Na MASS NMR spectra indicate the presence of a mobile sodium species, as well as a less mobile component confined in the polymer matrix. The sodium ions coordinate with carboxylate functionalities within the polymer matrix when dehydrated.

ACKNOWLEDGEMENTS

RT acknowledges fellowship support from the IBM corporation. RT and HL acknowledge support provided by the Office of Naval Research. JER acknowledges a grant from the Division of Materials Research at NSF through the Solid State Chemistry program (grant # DMR-8553275). Additional support to JER through the NSF Presidential Young Investigator program was obtained from Doty Scientific, Electronic Navigation Industries, The Exxon Education Foundation, General Electric Corporate Research and Development, General Electric NMR Instruments, IBM Instruments, Merck Sharp and Dohme, and The Monsanto Company.

REFERENCES

(1) Leidheiser, H., Jr. Inter. J. Adhesion Adhesives 1987,1. 1983, 103.

(2) Cypher, G. ACS Polymer Reprint 18 1977, 1, 482.

(3) Mayne, J. E. O.; Mills, D. J. J. Oil Col. Chem. Assoc. 1975, 58, 155.

(4) Leidheiser, H. Jr.; White, M. L.; Mills, D. J. EPRI Report, Cs-5449, Oct. 1983, 103.

(5) White, M. L.; Mills, D. J.; Leidheiser, H., Jr. Proc. Sym. Corrosion Protection by Organic Coatings, M. W. Kendig and H. Leidheiser, Jr., Eds., Electrochem. Soc. Vol. 87-2, 1983, 203.

(6) Mills, D. J., unpublished work, Lehigh University.

(7) Parks, J.; Leidheiser, H., Jr. Ind. Eng. Chem. Prod. Res. Dev. 1986, 25, 1.

(8) Leidheiser, H., Jr.; Vértes, A.; Czakó -Nagy, I.; Farkas, J., J. Electrochem. Soc. 1987, 134, 823.

(9) Leidheiser, H. Jr.; Czakó-Nagy, I.; Vértes, A. J. Electrochem. Soc. 1987, 134, 1470.

(10) Leidheiser, H. Jr.; Funke, W. J. Oil Col. Chem. Assoc. 1987, 70, 121.

(11) Gerstein, B. C.; Dybowski, C. R. "Transient Techniques in NMR of Solids", Academic Press, Inc.: Orlando, Florida, 1985; pg 8-11.

(12) ASTM Standard G8-79, "Annual Book of ASTM Standards, Vol. 06.01, Paint-Tests for Formulated Products and Applied Coatings", American Society for Testing and Materials, Philadelphia, PA, 1985, 1058.

(13) Leidheiser, H., Jr. Corrosion 1983 39, 189.

(14) Leidheiser, H., Jr. Prog. Org. Coatings 1983, 11, 19.

(15) Bloch, F. Phys. Rev. 1946, 70, 460.

(16) Rance, M. A.; Byrd, R. A. J. Magn. Res. 1983, 52, 221.

(17) Farrar, T. C.; Becker, E. D. "Pulse and Fourier Transform NMR-Introduction to Theory and Methods", Academic Press, Inc.: New York, 1971.

(18) Carr, H. Y.; Purcell, E. M. Phys. Rev. 1954, 94, 630.

(19) Meiboom, S.; Gill, D. Rev. Sci. Instrum. 1958, 29, 688.

(20) Pines, A.; Gibby, M.; Waugh, J. S. J. Chem. Phys. 1973, 59, 569.

(21) Earl, W. J.; VanderHart, D. L. J. Magn. Res. 1982, 48, 35.

(22) Venkatachalam, C. M.; Urry, D. W. J. Magn. Res. 1980, 41, 313.

(23) Deck, P. PhD Thesis, Lehigh University 1988.

(24) Opella, S. J.; Frey, M. H. J. Am. Chem. Soc. 1979, 101, 5854.

CORROSION INHIBITION OF STEEL BY LEAD PIGMENTS

I. THE STEEL-LEAD GALVANIC COUPLE IN ACETATE SOLUTIONS

John I. Mickalonis and Henry Leidheiser, Jr.

Note: This paper has been accepted for publication in CORROSION.

ABSTRACT

The corrosion behavior of lead-steel couples in acetate solutions is a function of pH. Steel is anodic to lead in an acidic acetate solution, whereas, lead is anodic to steel in an alkaline solution. This polarity reversal is attributed to the breakdown of the oxide on steel in the low pH solution. The corrosion process is under cathodic control in both acidic and alkaline solutions. Transport of oxygen to the cathode surface is the rate limiting step in the acidic solution. The corrosion process is under activation control in the alkaline solution.

INTRODUCTION

Lead pigments, such as litharge (PbO) and red lead (Pb_3O_4), are effective as corrosion inhibitors of steel in organic coating systems. Environmental concerns have limited the use of lead compounds (1) and have forced paint formulators to use different inhibitors. The majority of such substitute inhibitors have been selected empirically. An extensive study has been undertaken in an effort to develop an experimentally-based hypothesis for the operative mechanism of corrosion inhibition by lead pigments.

The inhibition by lead pigments has been attributed to several possible mechanisms which are important once a water phase has formed at the steel/coating interface. Lindqvist and Vannerberg (2) have summarized these mechanisms. The controlling mechanism may depend on the local interfacial environment. Inhibition is proposed to result primarily from: 1) the formation of lead-based deposits from soluble lead species, 2) an autocatalytic process of lead deposition and oxidation concurrent with the repair of the protective oxide on the steel surface, and 3) the alkaline properties of lead pigments in an aqueous phase. Studies by Mayne and coworkers (3-8) and Pryor (9) have shown that the inhibition mechanisms 1) and 3) were operative, although the structure and composition of the deposits were not fully identified. Mechanism 2), the autocatalytic process, has not been shown to be operative under conditions at the steel/coating interface.

The present study is concerned with the role of metallic lead and lead ions in corrosion inhibition at the steel/coating interface. Corrosion beneath organic coatings involves discrete anodic and cathodic sites. The pH of the aqueous phase near cathodic sites is as high as 13-14 when a cathodic potential is applied (10). For blisters formed under anodic conditions, the pH of the aqueous phase is reported to be around 4 (11). Also, the pH in a steel crevice where the crevice serves as the anode is in the range of 4-5.

In this study, solution pH values of 5 and 10 were chosen to simulate the aqueous phase under a coating near anodic and cathodic regions on the metal surface.

The anion of the aqueous phase under the coating may be a constituent leachable from the coating since anions appear to move through organic coatings at lower rates than alkali metal cations. Many protective coatings contain carboxyl groups (7) and coating and corrosion processes often develop such groups in the vicinity of the metal surface (12,13,14). Sodium acetate was thus selected as the electrolyte since the pH could be altered by the addition of acid or base without precipitation of the anion. Other anions have not been included in order to simplify the system and to focus on the interactions between lead and steel.

The mechanism by which lead inhibits the corrosion of steel may involve the interactions of the anodic and cathodic regions on the steel surface with metallic lead, solid lead compounds and soluble lead species. This paper is concerned solely with steel-lead galvanic couples in acetate media. The significance of the results to a better understanding of corrosion inhibition by lead pigments will be discussed, along with other data, in subsequent papers.

EXPERIMENTAL

Steel electrodes were made from a 0.025 cm thick, low-carbon steel sheet (ASTM 336, Q-Panel Co.) that was sheared to a size of 2 x 3 cm. Electrical connections were made with a multi-strand, 20-gauge copper wire that was soldered on one end. The electrodes and contact wires were coated with a hydrocarbon-based wax (Apiezon W) so that an area of 1-1.5 cm^2 was exposed. After the electrodes were constructed, the exposed surfaces were washed with a mild detergent, rinsed with distilled water and blown dry. The electrodes were stored in a desiccator for no longer than several days.

The lead electrodes were cut into disks from a 0.020 cm thick sheet with a composition of 99.9% Pb (Fisher Scientific). A disk was cleaned by soaking in a solution of saturated ammonium acetate for one day, rinsing with acetone and ethyl alcohol, and blowing dry. Samples were prepared immediately before testing. The sample holder supplied with the EG&G PAR K-47 Corrosion Cell was used with a sample surface area of 1 cm^2.

Measurements were performed in stirred solutions of 0.1M $NaC_2H_3O_2$ prepared from a reagent grade chemical (Fisher Scientific) and distilled water. The solution pH was adjusted to either 5 with glacial acetic acid or 10 with sodium hydroxide. Solutions were opened to the atmosphere without forced aeration unless otherwise noted.

The interactions between lead and steel were studied using galvanic coupling test, potentiodynamic polarization and weight loss measurements. The electrochemical tests were performed with either an EG&G PAR Model 350 Corrosion Measurement Console or an EG&G PAR 173 potentiostat controlled by PAR Model 332 SoftCorr^{TM} software on an Apple IIe computer.

The galvanic coupling tests were run in a 1000 ml beaker open to the atmosphere. The electrodes were of similar areas (1 cm^2) and placed 2.5 cm apart. A saturated calomel electrode (SCE) was used as the reference elec-

trode and was placed midway between the lead and steel electrodes. Tests were initiated either immediately after the electrodes were immersed or after the open-circuit potential of each electrode had stabilized. The duration of each test was 24 hours. The potential and current were monitored with the PAR 350 which was set up as a zero resistance ammeter. Several coupling tests were run under deaerated conditions in which argon was bubbled through the solutions for 30 minutes prior to the test. A rubber stopper was used to seal the top of the beaker.

Potentiodynamic polarization curves for lead and steel were obtained under similar test conditions to those that were used for the galvanic coupling test. Graphite rods and a SCE were used as the counterelectrode and reference electrode, respectively. Scans were initiated from the open-circuit potential after the electrode had stabilized. The scan rate was 0.1 mV/sec in the case of steel electrodes. The polarization curves for lead were sensitive to scan rate; the anodic curves were obtained at 0.5 mV/sec and cathodic curves at both 0.1 and 1.0 mV/sec. All reported potentials are versus the SCE.

Weight loss measurements were made for both coupled and uncoupled electrodes. Immersion tests for the uncoupled electrodes were performed when lead and steel electrodes were immersed in the same solution, as well as in separate solutions. The open-circuit potential of an uncoupled electrode was monitored during some of the tests. After the test, the electrodes were cleaned of their corrosion products and reweighed. The steel electrodes were cleaned according to ASTM G1-81. The corrosion products for the lead electrodes were removed by dabbing the exposed surface with a saturated ammonium acetate solution after which the electrodes were rinsed with ethyl alcohol and blown dry.

RESULTS

The open-circuit potentials of lead and steel change with the solution pH such that a polarity reversal occurs on changing the solution pH from 5 to 10. In the pH 5 solution, steel is anodic to lead; whereas in the pH 10 solution, lead is anodic to steel. The potential relationship for uncoupled electrodes in each solution is maintained over a 24-hour period as shown in Table 1 by the initial and final open-circuit potentials from typical experiments. The potential relationships are also maintained for a 24-hour period when the electrodes are coupled, i.e., a polarity reversal does not occur due to coupling. Table 2 shows the average open-circuit potentials of lead and steel electrodes from several coupling tests.

TABLE 1. Potential-Time Results: Initial and 24-Hour Values of the Potentials of Uncoupled Electrodes

Electrode	Solution pH	Potential (mV)[1] Initial	24-Hour
lead	5	-508	-508
steel	5	-585	-610
lead	10	-567	-473
steel	10	-255	+35

1. The potentials are typical values for each electrode.

TABLE 2. Galvanic Current Densities and Potentials for Lead-Steel Couples[1]

pH	Galvanic Current Density ($\mu A/cm^2$)	Galvanic Potential (mV) Initial	Galvanic Potential (mV) Final	Open-Circuit[2] Potential (mV) Steel	Open-Circuit[2] Potential (mV) Lead
5	225 (260)	-601 (-610)	-600 (-605)	-624	-502
10	21 (28)	-518 (-505)	-437 (-445)	-82	-458

1. Parenthetic values are predicted from the overlap of the anodic and cathodic polarization curves.

2. Potential measurements were made one minute after disconnecting couple.

The test results from the galvanic coupling tests indicate that the corrosion process of a lead-steel couple changes with the solution pH. Table 2 displays the average galvanic current density and the initial and final galvanic potentials for each solution pH. The parenthetic values are predicted from the overlap of the anodic and cathodic polarization curves. The galvanic current densities differ by an order of magnitude for the two solution pH values which is a consequence of the rate-controlling mechanism. Since the galvanic potential is close to that of the anode in each case, the corrosion process is under cathodic control.

The variations of the galvanic current density and potential were reproducible among tests at the same pH, but differed between the two solution pH values. For the pH 5 solution, the galvanic current density did not vary significantly from the average value with short-term fluctuations of approximately 10%. Similarly, the galvanic potential was also constant within a range of ±4 mV. At the start of the test, the potential was usually 5-10 mV

more active than the values reported in Table 2. The values as a function of time are shown in Figure 1. For the pH 10 solution, the galvanic current density and potential changed smoothly over the test period without significant short-term fluctuations. The current density started out high and dropped through a minimum before reaching a plateau. The potential asymptotically approached a constant value from a more active potential. Figure 2 shows these changes with time.

The weight loss measurements were made on both coupled and uncoupled electrodes. The average values for several tests are given in Table 3. The weight losses reported for the uncoupled electrodes are the average of those exposed in both the same and separate solutions since their values were similar. For the pH 5 solution, a comparison between the coupled and uncoupled weight losses shows that the lead is cathodically protected and the dissolution of the steel is accelerated. For the pH 10 solution, lead dissolution increases with coupling while dissolution of the steel is negligible. The weight losses of the coupled and uncoupled electrodes are consistent with the potential relationships of lead and steel.

TABLE 3. Weight Loss Measurements of Coupled and Uncoupled Electrodes

	Wt. Loss of Coupled Samples (mg/cm^2)[1]		Wt. Loss of Uncoupled Samples (mg/cm^2)[2]	
pH	lead	steel	lead	steel
5	0.3	12.6	27.1	7.8
10[3]	2.7	-0.6	1.4	<-0.1

1. Weight losses of coupled electrodes are the average of three tests.
2. Weight losses of uncoupled electrodes are the average of four tests.
3. Minus sign indicates a weight gain.

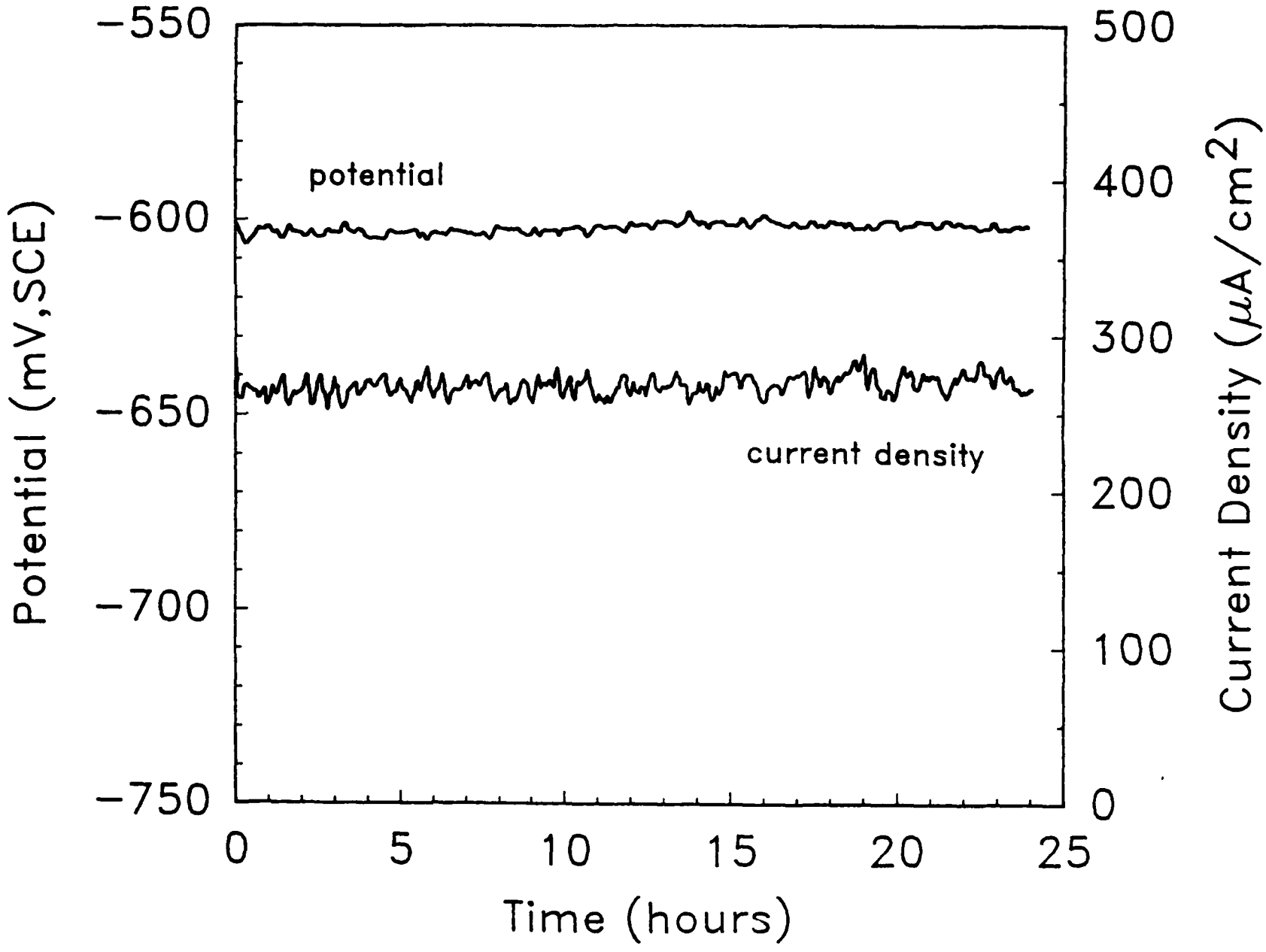

Figure 1. Galvanic current density and potential as a function of time over a 24-hour test in 0.1M sodium acetate, pH 5.

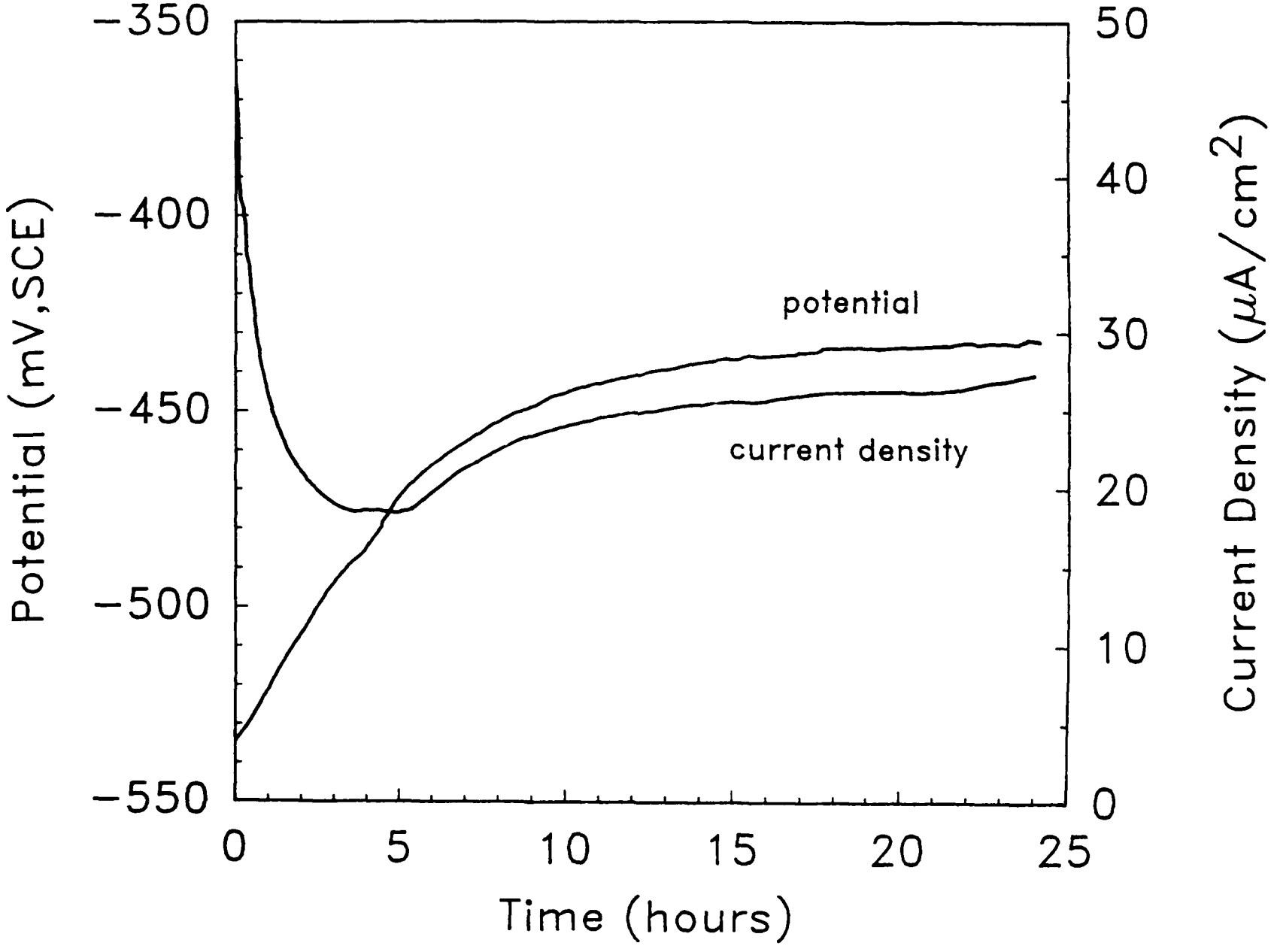

Figure 2. Galvanic current density and potential as a function of time over a 24-hour test in 0.1M sodium acetate, pH 10.

Visual observations were made of the corroded electrode surfaces from the galvanic coupling and immersion tests. Uncoupled lead and steel electrodes had roughened surfaces when exposed to the pH 5 solution. A loosely-adherent, blue-grey, corrosion product layer formed on the lead surface. The surface was etched below this layer. When coupled, the lead darkened slightly but maintained a metallic appearance as might be expected since the weight loss data indicate that lead is cathodically protected. Coupled and uncoupled steel electrodes developed a roughened, dark surface. A small area was also attacked around the perimeter of the exposed area beneath the wax. In the pH 10 solution, lead electrodes developed a white corrosion product layer when either coupled or uncoupled. X-ray diffraction showed this layer to be composed of lead oxide hydrate and lead carbonate hydroxide. The formation of this layer may be related to the ennoblement of the open-circuit potential of lead as shown in Tables 1 and 2. Coupled and uncoupled steel electrodes maintained their initial shiny metallic appearance.

The anodic and cathodic polarization curves of lead are shown in Figures 3 and 4 for the two solutions. The polarization curves are of the same general shape for both solution pH values. Anodically, lead displays active dissolution at low overpotentials as shown in Figure 3. A limiting current density is approached at larger overpotentials which may be due to the uncompensated solution resistance. The slight shoulder in the anodic curve for the pH 10 solution may be related to the white corrosion product layer reported above. The cathodic reaction on lead is the oxygen reduction reaction and a limiting current density is achieved at small overpotentials. At larger overpotentials the rise in current density is a consequence of the hydrogen reduction reaction as indicated by the evolution of gas from the surface. In the pH 10 solution, the cathodic curve at low overpotentials is a function of the scan rate. As shown in Figure 4, at a rate of 1.0 mV/sec a small Tafel-like

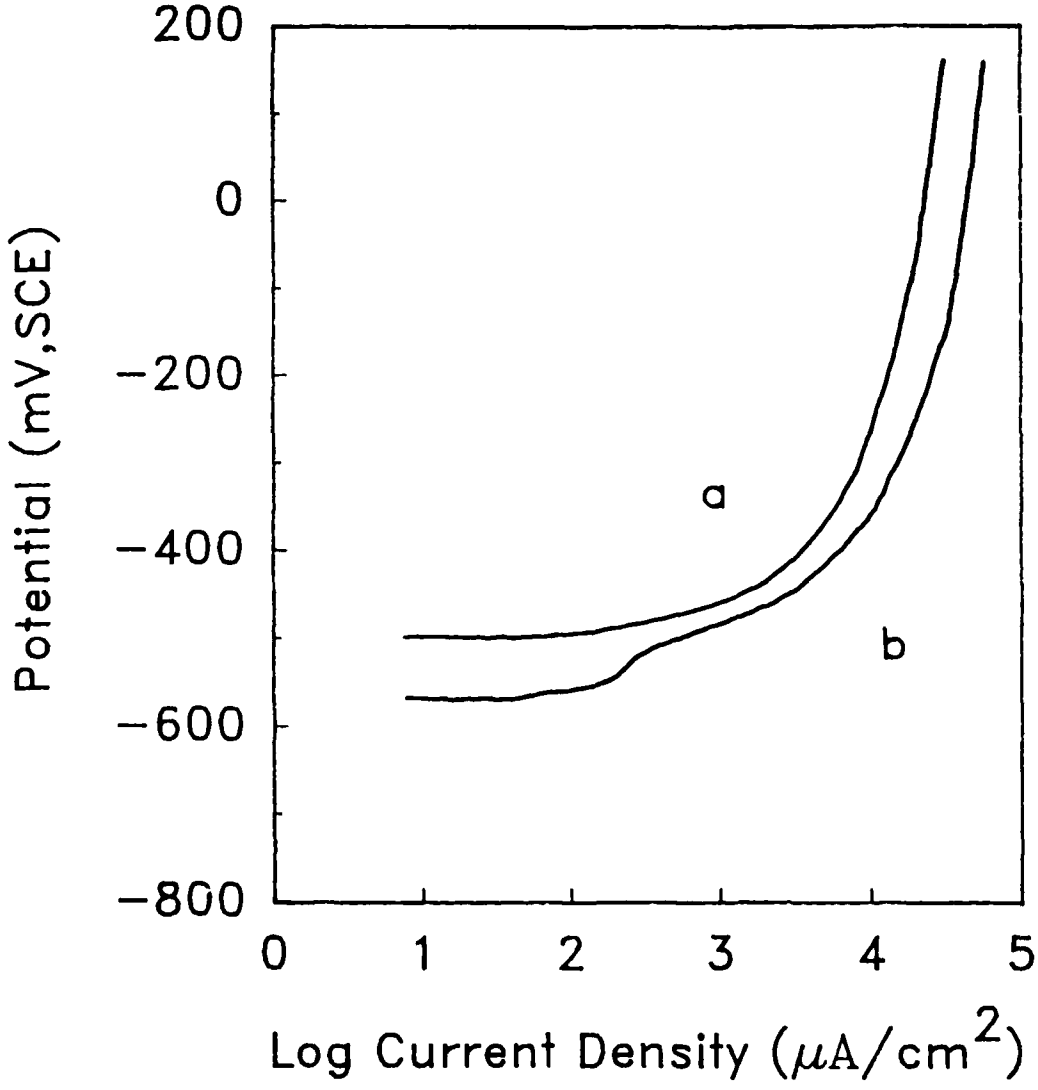

Figure 3. Anodic polarization curves for lead in 0.1M sodium acetate: a) pH 5, b) pH 10. Scan rate 0.5 mV/sec.

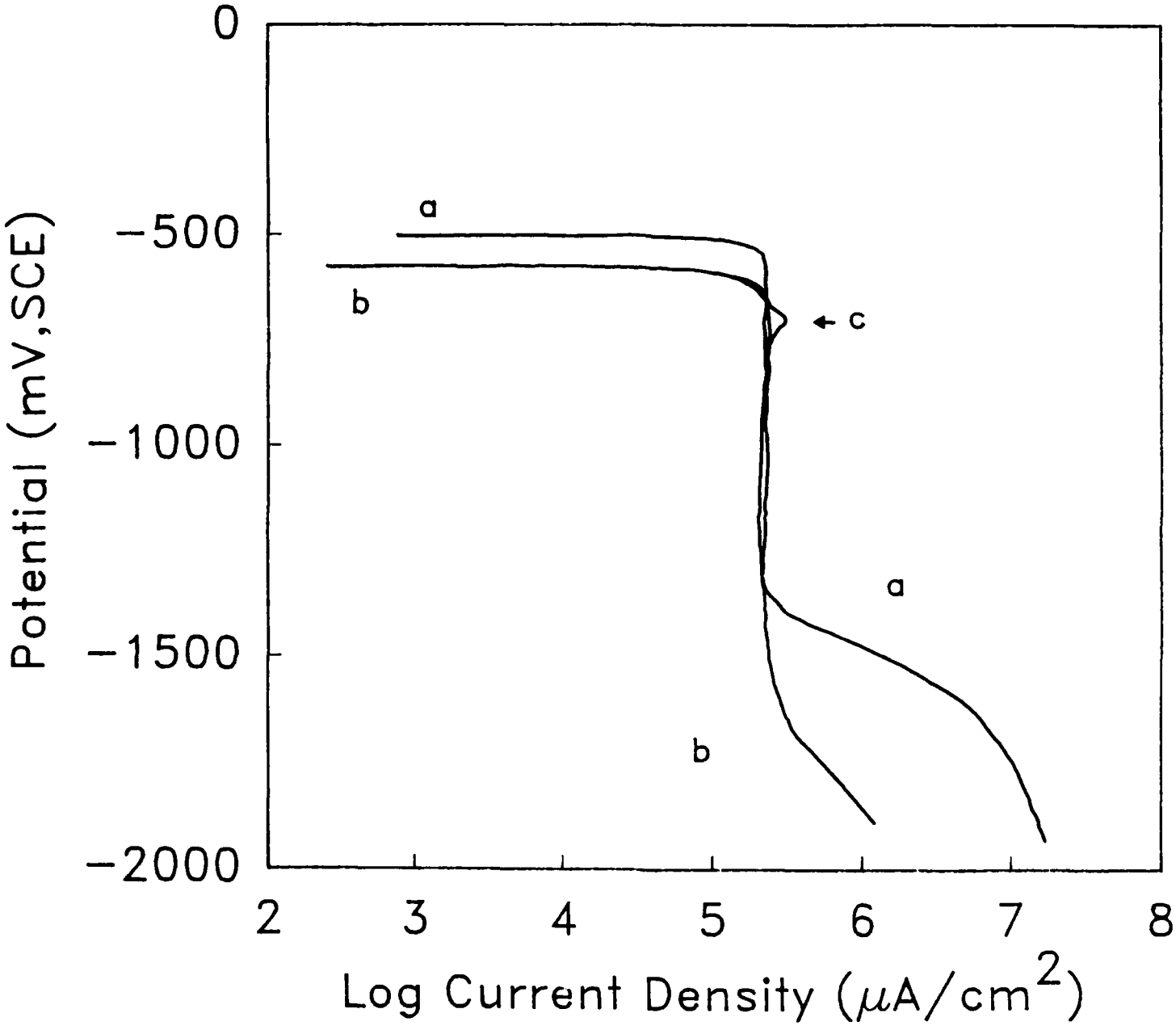

Figure 4. Cathodic polarization curves for lead in 0.1M sodium acetate: a) pH 5, scan rate 0.1 mV/sec; b) pH 10, scan rate 0.1 mV/sec c) pH 10, scan rate 1.0 mV/sec.

region is followed by a slight reduction peak. These features are absent at the slower scan rate of 0.1 mV/sec. The slower scan rate allows the oxide to be reduced at smaller overpotentials, thereby increasing the current density.

Polarization curves are given in Figures 5 and 6 for steel electrodes in the pH 5 and pH 10 solutions, respectively. The anodic curve indicates active dissolution in the pH 5 solution until a critical current density is reached at which the electrode passivates. The cathodic curve represents oxygen reduction at low current densities and hydrogen reduction at higher current densities. The reason for the shoulder that appears at -900 mV is unknown. In the pH 10 solution, the anodic curve has a low passive current density which increases slightly at larger overpotentials. Transpassive behavior occurs at more positive potentials. The cathodic reaction is the oxygen reduction reaction. Tafel behavior is displayed before a limiting current density is achieved at larger overpotentials. The Tafel slope is 116 mV/decade. A slight reduction peak is superimposed on this Tafel region. A film thickness of 50 Å was calculated from the amount of charge within the reduction peak assuming that the film was an oxide.

The oxidation or reduction of the acetate anion should not be seen for the potentials and current densities used in these tests. The anodic oxidation of acetic acid would occur by the Kolbe process at potentials greater than 2.1 V versus the normal hydrogen electrode (15). Carboxylic acids such as acetic acid are not easily reduced. Polarographic results (16) in an aqueous medium have shown half-wave potentials of -1.76 versus SCE.

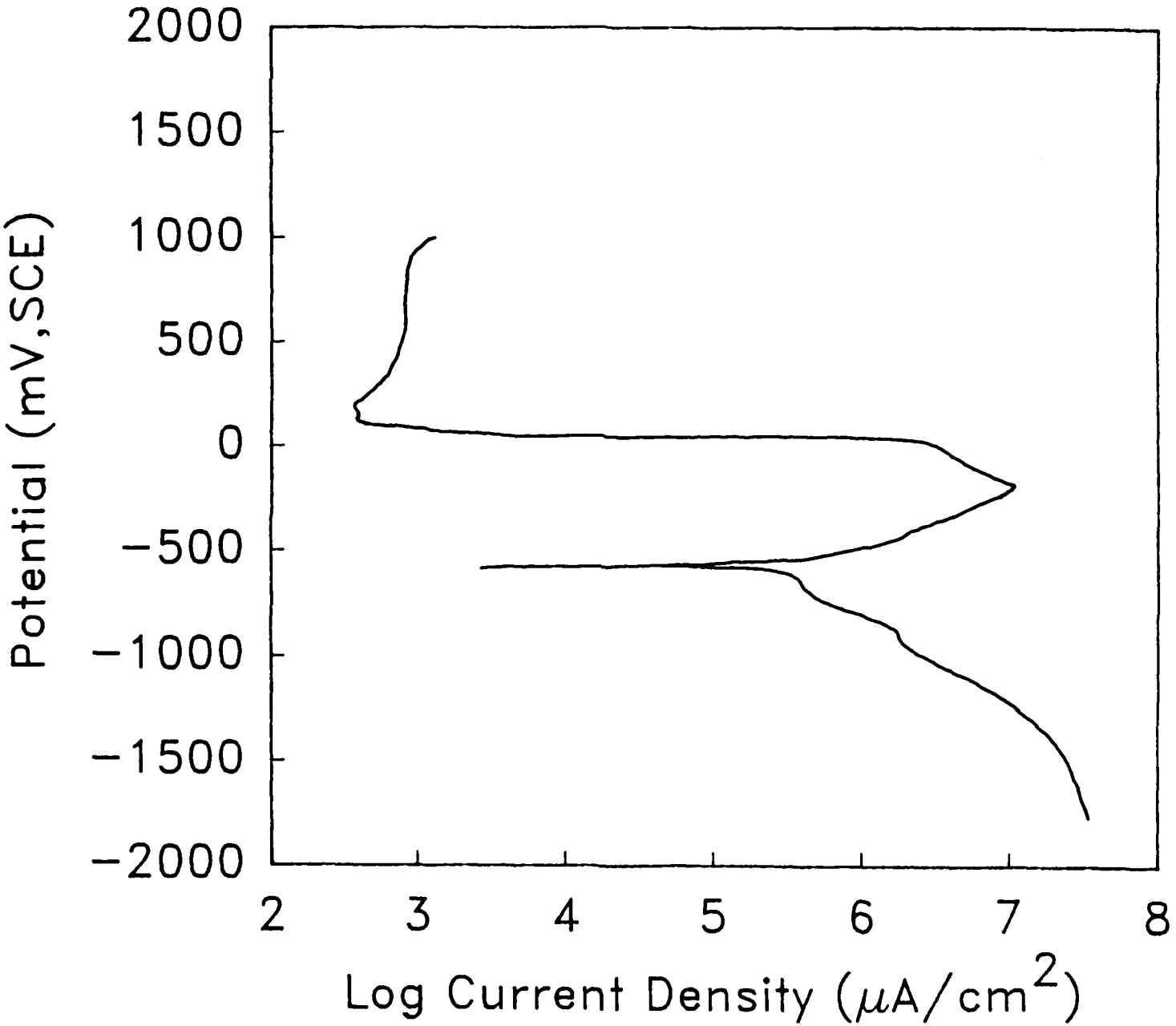

Figure 5. Anodic and cathodic polarization curves for steel in 0.1M sodium acetate, pH 5.

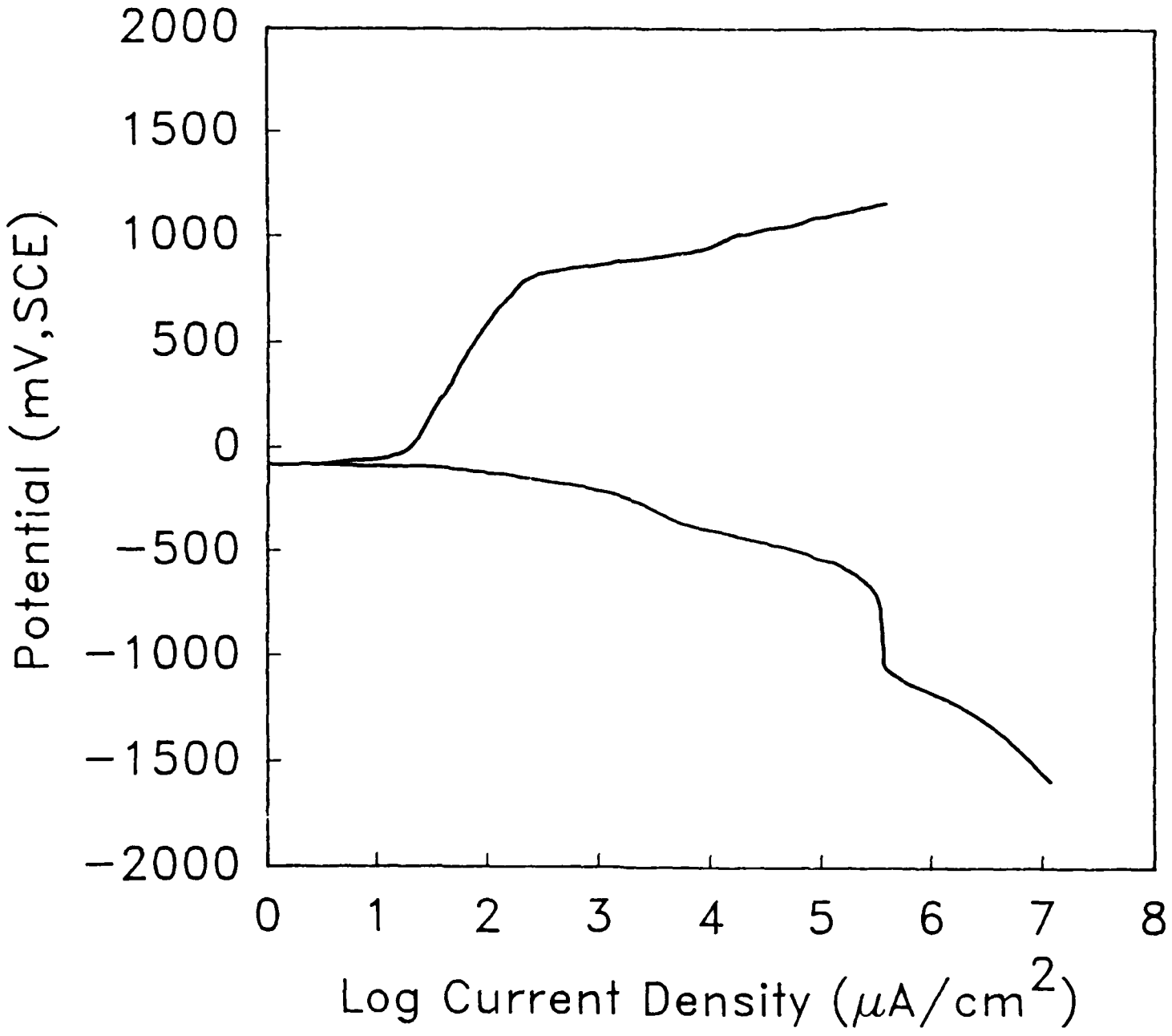

Figure 6. Anodic and cathodic polarization curves for steel in 0.1M sodium acetate, pH 10.

DISCUSSION

The polarity reversal of a lead-steel couple in sodium acetate solutions results from the presence or absence of a protective oxide on the steel surface. When a steel electrode is immersed in the pH 5 solution, the potential is initially more noble than -200 mV, but quickly achieves the more active values shown in Table 1. The change in potential is probably indicative of the removal (or partial removal) of the air-formed oxide. The steel became the anode in the pH 10 solution when deaerated with argon since a sufficient concentration of oxygen was not available for maintenance of the oxide layer.

The corrosion process of a lead-steel couple also changes with the solution pH. The intersection of the anodic and cathodic polarization curves for the uncoupled electrodes is useful for analyzing the controlling process, i.e., diffusion or activation control. In the pH 5 solution, the anodic curve for steel intersects the lead cathodic curve along the region of the limiting current density for oxygen reduction. The current density and potential at this point of intersection are similar to the experimental galvanic values. The parenthetic values in Table 2 are the average values taken from the overlap. In the pH 10 solution, the anodic curve for lead intersects the steel cathodic curve near the end of the Tafel region before the onset of the limiting current density. The controlling process is thus proposed as activation control of a step in the reduction of oxygen. The experimental and predicted values are also in good agreement for the high pH solution as shown in Table 2.

Corrosion current densities were determined from the extrapolation of the cathodic polarization curves back to the open-circuit potential. For lead in the pH 10 solution, the curve determined with a scan rate of 1.0 mV/sec was used. Weight loss values for the uncoupled electrodes were also converted to corrosion current densities. Since weight gains were found for steel in the

high pH solution, a corrosion current density was not calculated. The calculated corrosion current densities are in good agreement for both lead and steel as presented in Table 4.

TABLE 4. Experimental and Calculated Corrosion Current Densities of Uncoupled Electrodes

Electrode	Solution pH	Current Density ($\mu A/cm^2$) Experimental	Calculated
lead	5	292	320
	10	146	143
steel	5	328	292
	10	---	---

The correlation of weight loss to the galvanic current density depends on the controlling mechanism and the degree of polarization of the coupled electrodes. Mansfeld and Parry (17) have treated theoretically this correlation for the cases which apply to the lead-steel couples. The weight loss or dissolution current density of the anode (i_d) in the case of diffusion control is given by:

$$i_d = i_L (1 + A_c/A_a), \qquad (1)$$

where i_L is the limiting current density, and A_c and A_a are the geometric areas of the cathode and anode, respectively. If i_L on the anode and cathode are similar, i_L is equivalent to i_g, the galvanic current density. If i_L is different for the two electrodes, Mansfeld and Parry have shown that:

$$i_d = i_g + i_{corr} , \qquad (2)$$

where i_{corr} is the corrosion current density of the anode.

From the polarization curves in the pH 5 solution, i_L for lead is 200 $\mu A/cm^2$ and for steel is 340 $\mu A/cm^2$. Therefore, equation (2) describes the relationship between the weight loss and i_g. Table 5 shows i_d calculated from

TABLE 5. Experimental and Calculated Dissolution Current Densities of Anode in Lead-Steel Couples

Solution pH	Anode	Current Density ($\mu A/cm^2$) Experimental	Calculated
5	steel	504	517
10	lead	29	27 - 36.5

equation (2) and from the weight loss of the steel electrode when coupled to lead. The good agreement between these two values is further support for the conclusion that oxygen transport to the lead electrode is the rate-controlling step in the corrosion of a lead-steel couple in the pH 5 solution.

For the pH 10 solution where the galvanic potential is near the open-circuit potential of the anode, i_d falls in a range that depends on i_g and i_{corr}; specifically,

$$i_g < i_d < i_g + i_{corr} \cdot \qquad (3)$$

Mansfeld and Parry assumed that the dissolution of the anode did not show Tafel behavior. The anodic polarization curve of lead is consistent with this assumption. Table 5 shows the dissolution current densities based on both equation (3) and the weight loss of the coupled lead electrodes. The weight loss value falls within the range determined by i_g and i_{corr}.

The corrosion process for a lead-steel couple in an alkaline solution is complex since cathodic reactions occur on both lead and steel. The slight anodic polarization of the lead electrode should reduce the rate of the cathodic reaction below that of the diffusion-controlled rate. Different rate-controlling processes could presumably occur at each surface, although activation control of a step in the oxygen reduction is most likely for both surfaces.

ACKNOWLEDGEMENT

The authors are grateful to the Office of Naval Research who provided support for this research.

REFERENCES

1. Tater, K. B., Mater. Perf., 26, 9 (1987).

2. Lindqvist, S. A., and Vannerberg, N.-G., Werks. Korros., 25, 740 (1974).

3. Mayne, J. E. O., J. Soc. Chem. Ind., 65, 196 (1946).

4. Mayne, J. E. O., and Turgoose, S., Br. Corros. J., 11, 204 (1976).

5. Mayne, J. E. O., Turgoose, S., and Wilson, J. M., Br. Corros. J., 8, 236 (1973).

6. Appleby, A. J., and Mayne, J. E. O., J. Oil Col. Chem. Assoc., 50, 897 (1967).

7. Mayne, J. E. O., and van Rooyen, D., J. Appl. Chem., 4, 384 (1954).

8. Mayne, J. E. O., and Page, C. L., Br. Corros. J., 7, 115 (1978).

9. Pryor, M. J., J. Electro. Soc., 101, 141 (1954).

10. Ritter, J. J., and Kruger, J., Surface Science, 96, 364 (1980).

11. Schwenk, W., Corrosion Control by Organic Coatings, H. Leidheiser, Jr. (ed), NACE, 1981, 103.

12. Dickie, R. A., Hammond, J. S., and Holubka, J. W., Ind. Eng. Chem. Prod. Res. Dev., 20, 339 (1981).

13. Watts, J. F., and Castle, J. E., J. Mat. Sci., 18, 2987 (1983).

14. Granata, R. D., Deck, P. D., and Leidheiser, Jr., H., Proc. 1987 Triservice Conf. Corrosion, F. H. Meyer, Jr. (ed), U.S. Air Force Academy, Colorado, May 1987, Vol III, 280-302 (1988).

15. Eberson, L., and Utley J., Organic Electrochemistry, M. M. Baizer and H. Lund (eds), Marcel Dekker, 1983, 437.

16. Eberson, L., and Utley J., Organic Electrochemistry, M. M. Baizer and H. Lund (eds), Marcel Dekker, 1983, 376.

17. Mansfeld, F., and Parry, E. P., Corrosion Science, 13, 605 (1973).

INHIBITION IN THE CONTEXT OF COATING DELAMINATION

Henry Leidheiser, Jr.

Note: This paper has been accepted for publication by the National Association of Corrosion Engineers for inclusion in a book on inhibitors.

ABSTRACT

Many protective polymeric coatings suffer delamination from a metal substrate when the coated metal is immersed in an electrolyte and the potential of the metal is cathodic to its normal corrosion potential. The delamination process is a consequence of the oxygen reduction reaction occurring beneath the coating. Inhibition requires limiting the access to the reaction site of any of the four required species: oxygen, water, cations and electrons. Other ways to reduce the severity of attack include reducing the pH at the interface between the coating and the metal, increasing the resistance of the interfacial bond to alkaline attack and mechanical interlocking of the coating to the substrate.

INTRODUCTION

The major thrust of this article is a discussion of the means for inhibiting the delamination of polymeric coatings on metals when the metal is polarized to a potential cathodic to its rest potential in the medium under study. Such an effect is known as "cathodic delamination" when a sizeable defect is present in the coating and "cathodic blistering" when no apparent defect is present. The effect is particularly important in pipeline coatings, coatings on ship hulls, adhesives used to bond polymers and metals, lithographic coatings subjected to electroless deposition of a metal in channels and holes, and in perforated coatings where the exposed metal is anodic to the metal under the coating. In all the above cases the metal under the coating is cathodic to its rest potential and the oxygen reduction reaction is thermodynamically feasible in an aqueous environment under the coating.

A summary article on the cathodic delamination of polybutadiene has been published [1] and the observations reported therein appear to be generally applicable to many different types of coatings on many different metallic substrates. The rate at which cathodic delamination occurs is a function of many variables. Those that have been identified [2] include: pretreatment before application of the coating, nature of the metal, nature of the coating, method of application of the coating, the ions present in the aqueous environment, the amount of oxygen dissolved in the aqueous environment, the temperature and the magnitude of the applied potential. An article has also been published on the cathodic blistering of two coatings [3].

The delamination process occurs as a consequence of the fact that the oxygen reduction reaction, $H_2O + 1/2O_2 + 2e^- = 2OH^-$, occurs beneath the coating. The pH under the coating may be as high as approximately 14 as shown by Ritter and Kruger [4]. The exact mechanism by which the coating loses adherence is not certain, but the following processes may play a role in

some systems:

(1) The high hydroxyl concentration may dissolve the oxide at the metal/polymer interface.

(2) The high hydroxyl concentration may attack the polymer at the interface.

(3) the high hydroxyl concentration may cause dewetting.

(4) The alkali metal ions may exchange with hydrogen at the interface and break the bonding between the metal and the polymer.

The exact mechanism of delamination is not important for the purposes of this article, but the precursor oxygen reduction reaction is critically important in terms of inhibition. It is also likely that the mechanism of delamination is a function of the particular metal/polymer system.

The descriptions that follow are largely a summary of conclusions drawn from work in the author's laboratory and the presentation is not designed to be a thorough review of published literature. Much of the better work on reduction of the severity of cathodic delamination has been done in industrial laboratories and much of this work remains in the proprietary area.

POSSIBLE MEANS TO INHIBIT CATHODIC DELAMINATION

Seven possible methods for inhibiting cathodic delamination will be discussed herein. These are:

(a) Prevent the formation of an aqueous phase at the interface.

(b) Prevent the access of alkali metal cations to the interface.

(c) Prevent the access of electrons to the interface.

(d) Prevent the access of oxygen to the interface.

(e) Prevent the development of a high pH at the interface.

(f) Make the coating bond, as well as the conversion coating at the interface, more resistant to alkali.

(g) Improve the mechanical interlocking of polymer and substrate.

The first five relate to reducing the rate at which the oxygen reduction reaction occurs; the sixth relates to the nature of the chemical bonding at the interface; and the latter is purely a method for retaining the coating in proximity to the metal. Each of these will be discussed separately.

Prevent the Formation of an Aqueous Phase at the Interface. It is obvious that in the absence of an aqueous phase no electrochemical reaction, and the oxygen reduction reaction in particular, can occur at the interface. When a defect, such as a scratch or impact perforation of the coating, is present, the liquid environment will be in contact with the interface at the periphery of the defect. Reaction can proceed laterally from the periphery underneath the coating. However, the development of a strong alkaline environment is less likely, because the periphery is in contact with the bulk liquid and convective and diffusion processes will cause mixing and a high pH is not achieved. In the case of no apparent defect, an aqueous phase must develop beneath the coating. Even in the case of a coating with a defect, there is evidence [5] that the delamination process occurs in advance of the intact boundary between the metal and the coating. The photograph in Figure 1 shows an example of blisters that form in advance of the delaminating front in the case of a photoresist on copper.

Aqueous phase development requires that there exist voids at the metal/coating interface that can serve as nucleation sites for the formation of an aqueous phase. Reduction in the probability that nucleation sites exist at the interface occurs when the coating material wets the surface so well that voids

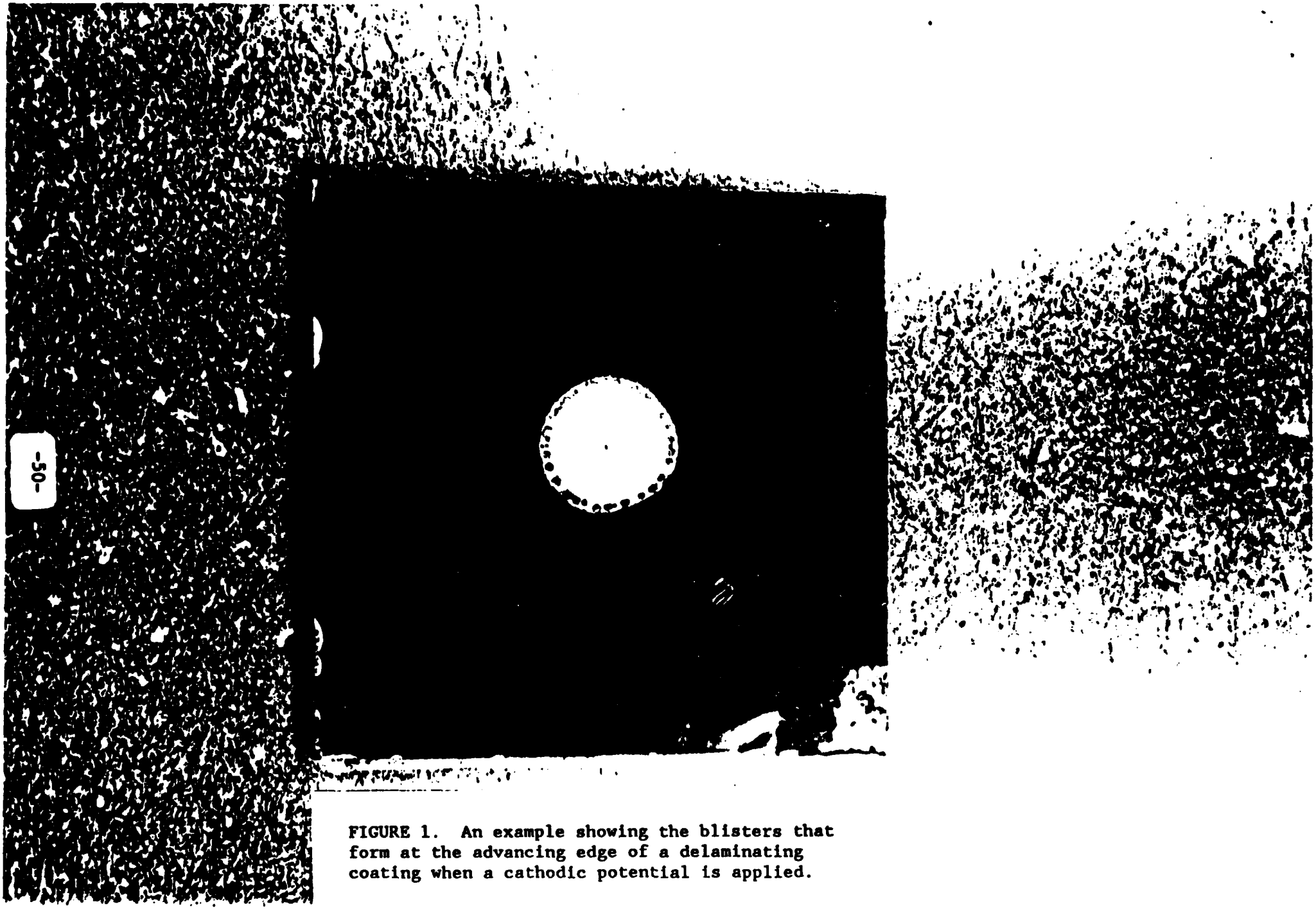

FIGURE 1. An example showing the blisters that form at the advancing edge of a delaminating coating when a cathodic potential is applied.

of small dimension do not exist. The importance of small-dimension imperfections at the metal surface is shown in the photograph in Figure 2 from a previous study [1], in which the shape of the cathodically delaminated region is elliptical with the major axis parallel to the direction of the polishing marks.

The reduction in the number of voids resulting from imperfect wetting of the metal by the polymer is brought about by any procedure that improves the wettability. The presence of imbedded abrasive particles, the presence of grain boundary depressions caused by pickling, the presence of crevices at the boundary of inclusions in the metal and the metal matrix all may result in the formation of voids, where water can readily nucleate under exposure to high relative humidity or immersion in water. Coatings in which there are present suitable wetting agents and in which the rheology is such that small crevices are readily penetrated will be less likely to cause the formation of voids at the interface. Coatings in which residual solvent exits the coating after polymerization and hardening have occurred are also prone to leave voids, in which water can condense.

Prevent the Access of Alkali Metal Cations to the Interface. The discussion is limited to alkali metal cations (Li^+, Na^+, K^+, Rb^+, Cs^+), since cathodic delamination occurs at a very low rate in the presence of other cations. Part of the reason for the ineffectiveness of other cations is that saturated solutions of their hydroxides have a much lower pH than those of the alkali metal cations.

It is a point of considerable controversy among workers in the field as to the method by which the alkali metal cation reaches the metal/coating interface. The author's work with coatings less than 100 μm in thickness suggests that the major route is through the coating [1]. Nuclear magnetic

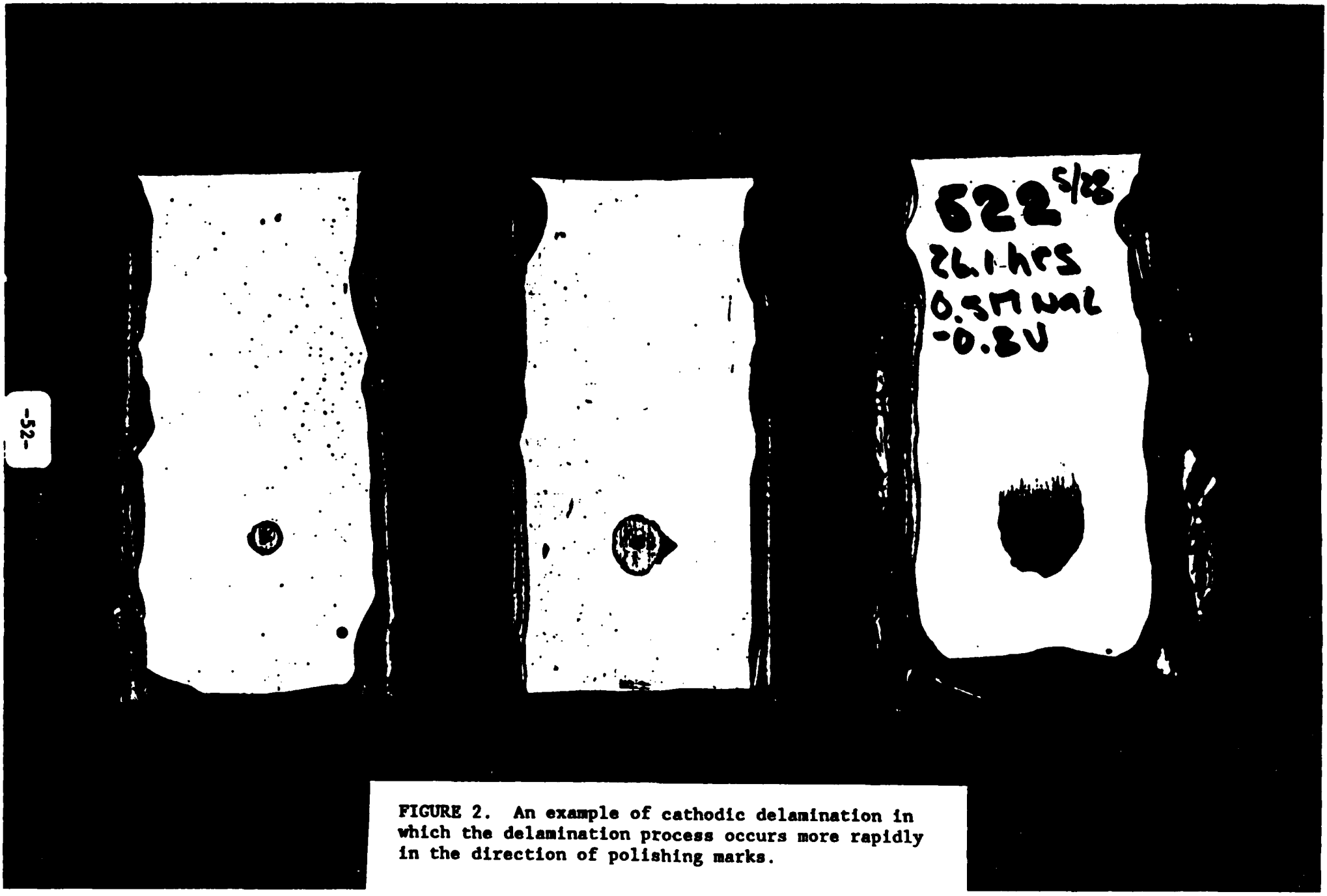

FIGURE 2. An example of cathodic delamination in which the delamination process occurs more rapidly in the direction of polishing marks.

resonance studies [6] and radiotracer measurements [7] give adequate proof that the alkali metal cations readily penetrate many types of coating when immersed in an aqueous solution and a cathodic potential is applied. In the case of very thick coatings it is likely that cations are also supplied from the edge of the defect. The presence of a delay time between the application of a potential and the onset of delamination in the case of thick coatings and the strong dependence of the rate of cathodic delamination on the thickness of the coating [2] are all suggestive that the main route is through the coating. The rate of cathodic delamination of all coatings studied in the author's laboratory decreases in the order $Cs^+ > K^+ > Na^+ > Li^+$, a relationship in accord with both the transference number of the cation and the diffusion coefficient in an aqueous solution. It is not known, however, if the same relationship exists in the rate of electromigration through a coating. It is known, however, that the application of a potential gradient increases the rate of migration of the cation through coatings [7].

Inhibition of cathodic delamination is possible in those situations where the cations present in the environment can be controlled. The substitution of alkaline earth metal cations in place of the alkali metal cations essentially will reduce cathodic delamination to a negligible rate under most conditions. It is recognized that this method of inhibition is impractical in those situations where the coated metal is exposed to sea water, to ground water or to run-off water that contains sodium chloride as a deicing agent.

Prevent the Access of Electrons to the Interface. An essential reactant in the oxygen reduction reaction is the electron. The source of the electron is the externally applied potential which supplies electrons to the metal. In order to be available for the reaction, however, the electrons must be available to components in the aqueous phase between the coating and the metal. Any film at the interface that has a low conductivity for electrons will

decrease the availability of electrons to the aqueous phase. Three examples from the author's work indicate the inhibiting nature of a low-conductivity film at the interface.

The rate of cathodic delamination from a coating on aluminum is very low relative to other metals when the applied potential is low. The resistive nature of the aluminum oxide on the surface of the aluminum prevents the transit of electrons when the applied potential across the oxide is low. The low rate of delamination of polybutadiene from aluminum agreed very well with the low rate of the cathodic reaction under a mild driving force [8].

Certain silanes when formed on a steel surface and subjected to water hydrolyze with the development of a surface film that has a low conductivity [9]. The rate of cathodic delamination from silane-coated surfaces is low, as shown in the example in Figure 3.

Doping of the surface oxide on zinc with small amounts of cobalt results in the formation of an oxide that is less active for the oxygen reduction reaction [10]. This reduced activity is very likely a consequence of the lower conductivity of the oxide. The lower rate of cathodic delamination of polybutadiene from the cobalt-doped oxide on zinc [1] is directly attributable to the lower activity of such a surface for the oxygen reduction reaction.

There are many ways in which the surface film on a metal may be made less conductive. Not all such methods are expected to be satisfactory in reducing the rate of cathodic delamination, because the bonding of the coating to the metal may be deteriorated and the intrusion of water at the interface may be accelerated. Such a system may exhibit poor water disbondment properties [11] and, consequently, may not perform well in service. Nonetheless, the development of surface films on the metal—a type of pretreatment—that have low conductivity represent a reasonable approach to inhibition of the cathodic delamination process.

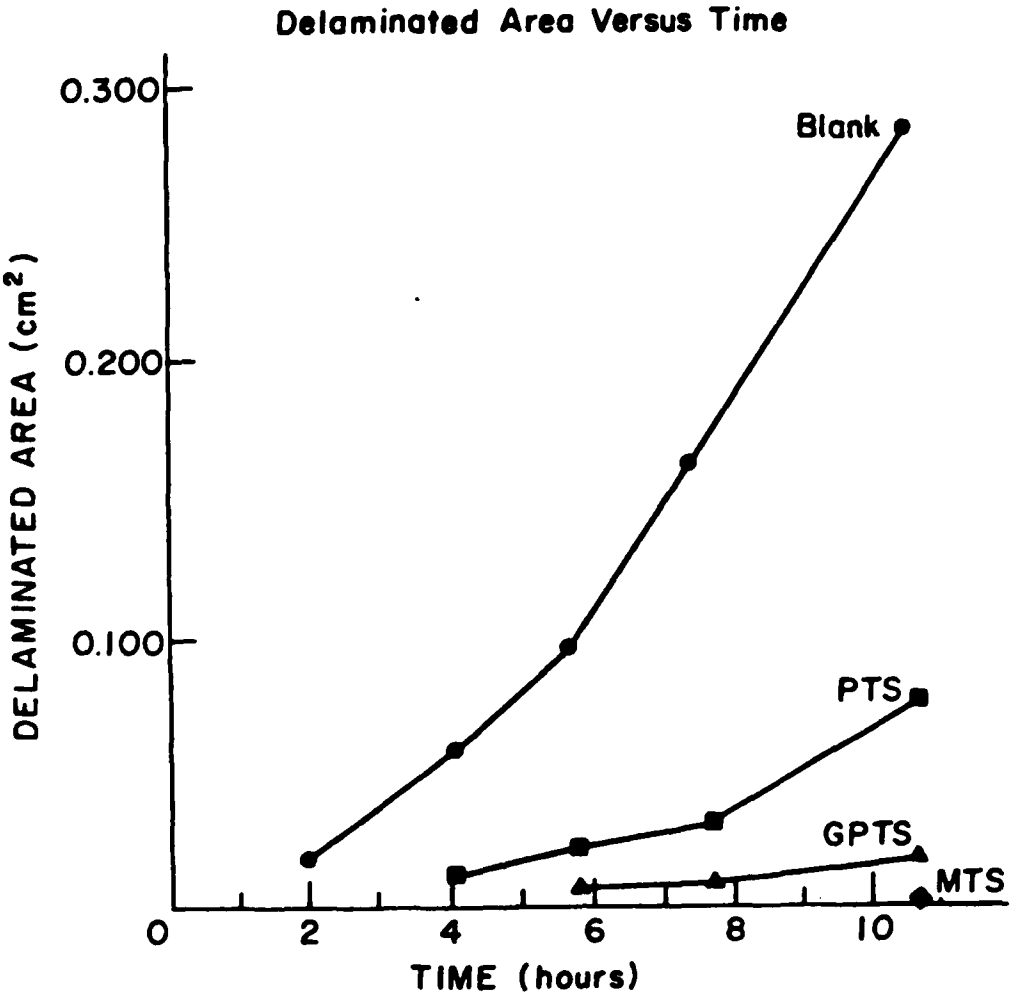

FIGURE 3. The rate of cathodic delamination of steel panels treated in phenyl trimethoxy silane (PTS), glycidoxy propyl trimethoxy silane (GPTS) and methyl triacetoxy silane (MTS) prior to coating with polybutadiene. Reference data for a non-silane treated panel coated with polybutadiene (blank) are also given.

Prevent the Access of Oxygen to the Interface. In the absence of oxygen the cathodic delamination of coatings occurs at a negligible rate [2]. The reason for this low rate is the fact that oxygen is an essential component of the oxygen reduction reaction and the reaction does not occur in the absence of oxygen. Since most, if not all, commercial coating systems are permeable to oxygen [12], the only satisfactory method to inhibit oxygen transport through the coating is to remove it from the environment. Similarly to the case of the cations, it is not possible to remove the oxygen from a sea water or underground environment. Inhibition of the reaction by removal of oxygen is only feasible in a closed system, where the user has control over the environment.

It may be possible to develop practical coating systems where oxygen transport is negligible or a coating system may be designed to scavenge oxygen. Neither possibility appears imminent.

Prevent the Development of a High pH at the Interface. The high pH that develops under the coating in the presence of alkali metal cations is a result of the fact that LiOH, NaOH, KOH, RbOH and CsOH are all very soluble and high concentrations of OH^- ions can form. Any components in the solution that are capable of reaching the interface and have the property of reducing the pH are potential inhibitors. The lower solubility of $Ca(OH)_2$, $Mg(OH)_2$ and $Ba(OH)_2$, for example, as compared to the alkali metal hydroxides is consistent with the fact that the rate of cathodic delamination is much lower in media containing salts of alklaline metal cations than in solutions of salts of alkali metal salts. Inhibition of cathodic delamination is thus possible in those cases where control of the ionic composition of the solution is practical.

Hydrogen ions can also serve as inhibitors as a consequence of the fact that the hydrogen ions can neutralize the hydroxide ions formed in the oxygen

reduction reaction. The rate of cathodic delamination is negligible in sufficiently acidic environments [13]. Inhibition is thus also feasible under conditions where the pH can be controlled. Unfortunately, this mechanism of inhibition is often not practical because of increased rates of corrosion of metallic components, the evolution of hydrogen and the consequent hazard, and the damage caused to the coating by the strong acid.

Make the Coating Bond, as well as the Conversion Coating at the Interface, More Resistant to Alkali. This mechanism of inhibition of the cathodic delamination process is favored by Hammond, Holubka, DeVries and Dickie [14]. These workers utilized X-ray photoelectron spectroscopy to determine the composition of the metal surface and the polymer surface after cathodic delamination. They studied the interfacial region, after separation, between an epoxy-ester, an epoxy-urethane, and an epoxy-amine and mild steel. They suggested that polymer degradation occurred at the interface because of the strong alkali generated by the cathodic reaction. Using phosphated steel as a substrate and a range of epoxy coatings [15], they confirmed the concept that coatings more resistant to attack by alkali had lower rates of cathodic delamination.

Many corrosion protective systems use a phosphate conversion coating between the metal and the coating. The phosphate is not continuous and bare metal spots are present among the phosphate crystals. These metal areas are the sites where water condenses and where the oxygen reduction occurs. Thus, alkali is generated in the immediate vicinity of the phosphate. The electron microprobe photographs of Iezzi [16] clearly show the dissolution of the phosphate, and the work of Sommer [17] has improved our knowledge of the mechanism of the dissolution and the effect of cations on the dissolution. The dissolution process breaks the bonding between the coating and the phosphate and the

adherence is lost. Phosphate conversion coatings with lower rates of dissolution in alkali represent a practical method for reducing the rate of cathodic delamination. It is apparent that any low solubility phosphate must also have the other physical properties required for high performance systems needed in automotive and appliance applications, for example.

Improve the Mechanical Interlocking of Polymer and Substrate. The bonding between a coating and a substrate involves chemical interactions in some cases [18] and mechanical interlocking in others. Sandblasting is reputed to improve the bonding because of the roughness of the substrate surface. Phosphate conversion coatings provide a very rough surface into which the polymer component of the coating penetrates. This rough surface tends to retain the coating in close proximity to the metal, even in those cases where the bond is broken in many places. The protective quality of the coating may be degraded but the coating may still provide some barrier protection. Mechanical interlocking retention of the coating to the surface should not be considered to represent a primary mode of resistance to cathodic delamination.

REFERENCES

1. H. Leidheiser, Jr., J. Adhesion Sci. Tech. Vol. 1, No. 1, p.79 (1987).

2. H. Leidheiser, Jr., and W. Wang, J. Coatings Tech. Vol. 53, No. 672, p.77 (1981).

3. V. S. Rodriguez and H. Leidheiser, Jr., J. Coatings Tech. Vol. 60, No.757, p.46 (1988).

4. J. J. Ritter and J. Kruger, in "Corrosion Control by Organic Coatings," H. Leidheiser, Jr., Ed., p. 28, Natl. Assoc. Corrosion Engrs., Houston, Texas (1981).

5. J. F. Watts and J. E. Castle, J. Mat. Sci. Vol. 18, p.2987 (1983).

6. R. Turoscy, J. Roberts and H. Leidheiser, Jr., submitted to J. Phys. Chem.

7. J. Parks and H. Leidheiser, Jr., Ind. Eng. Chem. Prod. Res. Dev. Vol. 25, p.1 (1986).

8. H. Leidheiser, Jr., Corrosion Vol. 38, p.374 (1982).

9. H. Leidheiser, Jr., M. De Crosta and R. D. Granata, Corrosion Vol. 43, p.382 (1987).

10. H. Leidheiser, Jr., and I. Suzuki, J. Electrochem. Soc. Vol. 128, p.242 (1981).

11. H. Leidheiser, Jr., and W. Funke, J. Oil Colour Chem. Assoc. Vol. 70, No. 5, p.121 (1987).

12. M. Yaseen and W. Funke, J. Oil Colour Chem. Assoc. Vol. 61, p.284 (1978).

13. M. L. White, H. Vedage, R. D. Granata and H. Leidheiser, Jr., Ind. Eng. Chem. Prod. Res. Dev. Vol. 25, p.129 (1986).

14. J. S. Hammond, J. W. Holubka, J. E. DeVries and R. A. Dickie, Corros. Sci. Vol. 21, p.239 (1981).

15. J. E. Devries, J. W. Holubka, and R. A. Dickie, Ind. Eng. Chem. Prod. Res. Dev. Vol. 22, p.256 (1983).

16. R. A. Iezzi and H. Leidheiser, Jr., Corrosion Vol. 37, p.28 (1981).

17. A. J. Sommer and H. Leidheiser, Jr., Corrosion Vol. 43, p.661 (1987).

18. H. Leidheiser, Jr., and P. D. Deck, Science Vol. 241, Sept. 2, p.1176 (1988).